[Submitted to the journal *Papers in Palaeontology* in july 29, 2019]

SYSTEMATIC REVISION AND REDEFINITION OF THE GENUS *SCIRROTHERIUM* EDMUND & THEODOR, 1997 (CINGULATA, PAMPATHERIIDAE): IMPLICATIONS FOR THE ORIGIN OF PAMPATHERIIDS AND THE EVOLUTION OF THE SOUTH AMERICAN LINEAGE INCLUDING *HOLMESINA*

By KEVIN JIMÉNEZ-LARA[1,2]

[1] División de Paleontología de Vertebrados, Museo de La Plata, Facultad de Ciencias Naturales y Museo, Universidad Nacional de La Plata, Paseo del Bosque s/n, B1900FWA La Plata, Argentina.

[2]CONICET, Consejo Nacional de Investigaciones Científicas y Técnicas, Argentina.

e-mail: kjimenezlara@fcnym.unlp.edu.ar

Abstract: The intrageneric relationships of the pampatheriid genus *Scirrotherium* and its affinities with supposedly related genera, i.e. *Kraglievichia* and *Holmesina*, are revised through parsimony phylogenetic analyses and new comparative morphological descriptions. For this work was analyzed unpublished material of pampatheriids (numerous osteoderms, one partial skull and a few postcranial bones) from Neogene formations of Colombia. The results show that *Scirrotherium* is paraphyletic if we include all its referred species, i.e. *Scirrotherium hondaensis*, *S. carinatum* and *S. antelucanus*. The species *S.*

carinatum is closer to *Kraglievichia paranensis* than to *S. hondaensis* or *S. antelucanus*, then it is proposed the new name *K. carinatum* comb. nov. The relationships between *S. hondaensis* and *S. antelucanus* could not be resolved, so these species should be designated in aphyly. In spite of failing to recover *S. hondaensis* and *S. antelucanus* as one single clade, here is preferred to maintain the generic name *Scirrotherium* in both species from diagnostic evidence. New emended diagnoses for *Scirrotherium*, *S. hondaensis* and *Kraglievichia* are provided. The genus *Holmesina* was found monophyletic and located as the sister clade of *Scirrotherium* + *Kraglievichia*. The evolutionary and biogeographical implications of the new phylogeny and taxonomical re-arrangements are discussed. It is claimed a possible geographical origin of the family Pampatheriidae and *Scirrotherium* in low latitudes of South America as early as Early Miocene (Burdigalian) times. The South American ancestor or sister taxon of *Holmesina* is predicted as morphologically more similar to *Scirrotherium* than to *Kraglievichia*.

Key words: Pampatheriidae, *Scirrotherium*, *Kraglievichia*, *Holmesina*, Great American Biotic Interchange, Neogene.

The pampatheriids (Pampatheriidae) are a morphologically conservative extinct clade of glyptodontoid cingulates or highly armored xenartrans (Glyptodontoidea *sensu* McKenna & Bell 1997) with medium-to-large body sizes (Edmund 1985; Góis et al. 2013). They were distributed from the Neogene to the Early Holocene in numerous localities of South America (their native range), Central America, Mexico and the United States (Edmund 1985; Vizcaíno et al. 1998; Rincón et al. 2014; Góis et al. 2015 and references there). As the modern armadillos (Dasypodidae), pampatheriids have a flexible carapace by the

presence of three transverse bands of imbricated osteoderms which conform a kind of "articulation" between the scapular and pelvic shields (Edmund 1985). The pampatheriids also have multiple features, especially in their skull and mandible, which, collectively, define them as the sister group of glyptodontids –Glyptodontidae (Gaudin 2004; Gaudin & Wible 2006; Billet et al. 2011; Delsuc et al. 2012), namely deep horizontal mandibular ramus, laterally-directed zygomatic root, transversely-wide glenoid fossa, rough pterygoids, among others (Gaudin & Wible, 2006).

The fossil record of Pampatheriidae is mainly represented by isolated specimens, of which most of them are osteoderms and, in lesser extent, skulls, mandibles and postcranial bones; fairly complete and articulated skeletons are uncommon (Edmund 1985; Góis 2013). Due the above, the systematics of this xenartran group has historically been based on osteodermal characters (Edmund 1985, 1987; Góis et al. 2013), as has been the case with other cingulate clades. Overall, nearly two tens of pampatheriid species and seven genera are known (Góis 2013). The latter conform two possible subfamilial lineages: (1) that including to the genera *Plaina* and *Pampatherium*; and (2) that comprising the genera *Scirrotherium*, *Kraglievichia* and *Holmesina* (Edmund 1985). However, it does not exist in the scientific literature a published phylogenetic analysis on the relationships between the different pampatheriid genera. Only Góis (2013) performed a phylogenetic analysis for these taxa, but his results have not been published. In Góis's consensus tree, it was corroborated the hypothesis by Edmund (1985) on the two subfamilial lineages.

The genus *Scirrotherium* is the oldest known pampatheriid in the fossil record (Góis et al. 2013; Rincón et al. 2014) and one of the four Miocene genera (the other ones are *Kraglievichia* Castellanos 1927; *Vassallia* Castellanos, 1927; and *Plaina* Castellanos,

1937). This taxon was originally described by Edmund & Theodor (1997) from craniomandibular, postcranial and osteodermal specimens collected in the Middle Miocene (Serravalian) sedimentary sequence of the La Venta area, southwestern Colombia. These authors interpreted that the only known species in that time and type species, *Scirrotherium hondaensis*, has plesiomorphic traits in its osteological morphology which are expected for its antiquity. Additionally, they highlighted morphological similarity of *S. hondaensis* with the species *Vassallia minuta* (Late Miocene of southern and central South America; De Iullis & Edmund 2002), more than with any other pampatheriid.

Later, Góis et al. (2013) described a second species for *Scirrotherium*, *S. carinatum*, from the Late Miocene (Tortonian) of northeastern and southern of Argentina-northwestern Brazil. In northeastern Argentina (Entre Ríos Province), *S. carinatum* shares basal stratigraphic levels ("Conglomerado Osífero", literally 'bone-bearing conglomerate') in the Ituzaingó Formation with the middle-sized pampatheriid *Kraglievichia paranensis* (Góis et al. 2013; Scillato-Yané et al. 2013), a taxon different but not distantly related to *Scirrotherium* as previously indicated. The species *S. carinatum*, based exclusively on osteoderms of different regions of the armored carapace, has a body size comparable or slightly smaller than that of *S. hondaensis* (Góis et al. 2013).

The phylogenetic analysis conducted by Góis (2013) recovered in polytomy to *S. carinatum* and *S. hondaensis*, being one of these species or both of them the sister taxon/taxa of the clade *Kraglievichia* + *Holmesina* (except *H. floridanus*). It is notorious the non-basal position of the *Scirrotherium* species within the general topology of the cladogram despite they conform the oldest known genus. Instead, these species are closely placed to widely recognized terminal taxa, i.e. *Holmesina* spp. (Edmund 1985, 1987; Gaudin & Lyon 2017).

If this result is correct, it would indicate a significantly long ghost lineage at the base of the evolutionary tree of Pampatheriidae.

Góis found phylogenetic support for *Scirrotherium* through one single synapomorphy, i.e. presence of deep longitudinal depressions (LDs) in osteoderms. This is a distinctive feature of *S. carinatum* but, in contrast, the LDs in *S. hondaensis* are relatively shallow, rather than deep. Interestingly, this putative synapomorphy is actually shared by *K. paranensis*. Góis explained the insufficient phylogenetic resolution in his analysis for *Scirrotherium* using the argument of fragmentary character of the fossil specimens of *S. hondaensis*, although in the case of *S. carinatum*, unlike the Colombian species, the skull, mandible and any postcranial bone are unknown (Góis et al. 2013).

Almost simultaneously to Góis's works, Laurito and Valerio (2013) reported and studied new pampatheriid material from the Late Miocene (Tortonian to Messinian) of Costa Rica, which was assigned to a new species, *S. antelucanus*. This species, the largest referred to *Scirrotherium* so far (body size comparable or slightly smaller than that of *K. paranensis*; Laurito & Valerio 2013), is based on osteoderms and some postcranial bones (femoral fragments and metatarsals). The occurrence of *S. antelucanus* in the Late Miocene of southern Central America suggests the genus *Scirrotherium* take part earlier than any other pampatheriid (i.e. *Plaina*, *Pampatherium*, *Holmesina*; Woodburne 2010) in the late Cenozoic biotic interchanges of the Americas with its invasion to tropical North America ("North America" is defined here as all the continental territories north of the ancient location of the main geographical barrier between the Americas during the early Neogene, i.e. the Central American Seaway in northwestern Colombia), before the definitive closing

of the Panama Land Bridge (PLB) ca. 3 mya (Schmidt 2007; Coates & Stallard 2013; O'dea et al. 2016; Jaramillo 2018).

Recently, in several contributions on fossil vertebrate assemblages from the Neogene of Venezuela and Peru has been reported the occurrence of isolated osteoderms referred to *Scirrotherium*. In basis to these discoveries, the geographical and chronological distribution of the genus has been expanded in such a way that this taxon is now known for the Early and Late Miocene (Burdigalian and Tortonian) of northwestern Venezuela (Rincón et al. 2014; Carrillo-Briceño et al. 2018) and Late Miocene (Tortonian) of northeastern Peru (Antoine et al. 2016).

Assuming all the previous taxonomical assignments are correct, the latitudinal range of *Scirrotherium*, from southern Central America to Patagonia (southern Argentina), is the widest latitudinal range of a Miocene pampatheriid, only comparable with those of the Plio-Pleistocene forms *Pampatherium* and *Holmesina* (Scillato-Yané et al. 2005). This biogeographical inference provides support to the hypothesis that *Scirrotherium* inhabited varied environments within its latitudinal range, and, consequently, it probably had a relatively high ecological flexibility (Góis et al. 2013).

Despite the progress in the systematic and biogeographical research of *Scirrotherium*, it is necessary at present a new reevaluation of several fundamental hypotheses about this taxon, including its taxonomical definition, monophyly and evolutionary relationships with other pampatheriid genera. Using parsimony phylogenetic analyses and morphological comparative descriptions of new pampatheriid remains from the Neogene of Colombia, this contribution reevaluates the taxonomic status of *Scirrotherium* and its relationships with supposedly allied genera, i.e. *Kraglievichia* and *Holmesina*. Accordingly, I suggest a new

136 taxonomical and nomenclatural reorganization with emended diagnoses for *Scirrotherium*
137 and, complementarily, for the genus *Kraglievichia*.

138 Finally, considering the systematic reanalysis, I depict a model of biogeographical
139 evolution for the lineage *Scirrotherium-Kraglievichia-Holmesina*. From this model, I draw
140 out new hypotheses on the geographical origin of Pampatheriidae and the late Cenozoic
141 dispersal events of pampatheriids to/from North America, including a possible re-entry
142 event to South America of the species *S. antelucanus*.

143

144 **MATERIAL AND METHODS**

145 **Selection of OTUs**

146 I studied 12 species of pampatheriids attributed to six different genera. These species, in
147 alphabetic order, are: *Holmesina floridanus* Robertson, 1976; *H. major* Lund, 1842; *H.*
148 *occidentalis* Hoffstetter, 1952; *H. paulacoutoi* Cartelle & Bohórquez, 1985; *H.*
149 *septentrionalis* Leidy, 1889; *Kraglievichia paranensis* Ameghino, 1888; *Pampatherium*
150 *humboldtii* Lund, 1839; *Plaina intermedia* Ameghino, 1888; *Scirrotherium antelucanus*
151 Laurito & Valerio, 2013; *S. carinatum* Góis, Scillato-Yané, Carlini and Guilherme, 2013; *S.*
152 *hondaensis* Edmund & Theodor, 1997; and *Vassallia minuta* Moreno & Mercerat, 1891. It
153 was also included in this selection unidentified pampatheriid material (MUN STRI 16718
154 and 38064; see the section *Institutional abbreviations*) from the Castilletes Formation in
155 Colombia (see below), which is referred as “Castilletes specimens”.

156 Among the former nominal species, I follow to Góis (2013) in considering *Vassallia*
157 *maxima* as a junior synonym of *Pl. intermedia*. The only one species of *Holmesina* not

158 included in this study was *H. rondoniensis* Góis, Scillato-Yané, Carlini & Ubilla, 2012.
159 This decision is based on a preliminary phylogenetic analysis in which *H. rondoniensis* was
160 identified as a "wildcard" taxon obscuring the phylogenetic resolution. It was also not
161 included in this analysis the species *Tonnicinctus mirus* Góis, González Ruiz, Scillato-Yané
162 & Soibelzon, 2015, which is considered a potentially problematic and late diverging taxon
163 without any apparent substantial interest with respect to the systematic issues here
164 addressed.

165

166 **Morphological description of the specimens**

167 The osteological morphology of the selected species was revised from direct observations
168 on specimens previously studied in other works, as well as through published/unpublished
169 descriptions (Simpson 1930, Castellanos 1937; Edmund 1985, 1987; Edmund & Theodor
170 1997; Góis 2013; Góis et al. 2013; Laurito & Valerio 2013; Scillato-Yané et al. 2013; Góis
171 et al. 2015; Gaudin & Lyon 2017). Naturally, according to the objectives of this research,
172 during the revision of material I focused on the species *S. antelucanus*, *S. carinatum* and *S.*
173 *hondaensis*, and, additionally, species of genera considered closely allied to *Scirrotherium*,
174 i.e. *K. paranensis* and *Holmesina* spp. (particularly *H. floridanus*; Appendix S1 of the
175 Supplementary Material).

176 On other hand, new undescribed cranial, postcranial and osteodermal specimens were also
177 used to reexamine the morphological variability of *Scirrotherium*. This material comes
178 from five Neogene geological units of Colombia (Fig. 1): (1) Castilletes Formation (Early
179 to Middle Miocene, late Burdigalian-Langhian), Municipality of Uribia, Department of La

Guajira; (2) La Victoria Formation (late Middle Miocene, Serravalian), Municipality of Villavieja, Department of Huila; (3) Villavieja Formation (late Middle Miocene, Serravalian), Municipality of Villavieja, Department of Huila; (4) Sincelejo Formation (Late Miocene-Early Pliocene, Messinian-Zanclean), Municipality of Los Palmitos, Department of Sucre; (5) Ware Formation (Late Pliocene, Piacenzian), Municipality of Uribia, Department of La Guajira. For detailed lithological descriptions and chronostratigraphic inferences on these formations, the reader is referred to the following references: Moreno et al. 2015 for the Castilletes and Ware Formations; Guerrero 1997, Flynn et al. 1997 and Anderson et al. 2016 for the La Victoria and Villavieja formations; and Flinch 2003, Villarroel & Clavijo 2005, Bermúdez et al. 2009 and Alfaro & Holz 2014 for the Sincelejo Formation. The new fossils are deposited at the Paleontological Collection of the Museo Mapuka de la Universidad del Norte, Barranquilla, Colombia, except those collected in the La Victoria and Villavieja Formations. The latter are housed at the Museo de Historia Natural La Tatacoa, La Victoria Town, Municipality of Villavieja, Department of Huila, Colombia.

Cranial measurements, all taken on the midline of the skull (dorsally or ventrally), follow Góis (2013). The anatomical terminology for osteoderms is based on the proposal of Góis et al. (2013). All the measurements were taken with a digital caliper with a precision of 0.01 mm.

Selection and codification of characters

I exclusively selected cranial, dental and osteodermal characters given that the postcranial bones of most species of Pampatheriidae is poorly known (Góis 2013). This selection was based on personal observations and previous quantitative and qualitative analyses of the interspecific, intergeneric and familial morphological variability of pampatheriids (e.g. Edmund 1985, 1987; Góis 2013; Góis et al. 2013; Laurito & Valerio 2013). Overall, a matrix of 27 characters (Appendix S2 of the Supplementary Material) was built and managed on Mesquite version 2.75 (Maddison & Maddison 2010). In this character list, 20 characters are parsimony-informative and 7 are parsimony-uninformative; 5 are osteodermal characters and 22 are cranial or dental. The parsimony-uninformative characters allow to define potential autapomorphies of the studied taxa.

Cladistic analyses

Parsimony analyses under schemes of equal weights and implied weights (characters reweighted *a posteriori*; see below) were performed in PAUP* version 4.0a142 (Swofford 2015). In both weighting schemes, the species *P. humboldtii*, *Pl. intermedia* and *V. minuta* were defined as outgroup. The monophyly of the outgroup and rooting of trees from it was constrained. The selection of the outgroup is based on the hypothesis about subfamilial relationships of Pampatheriidae by Edmund (1985). The characters were treated as unordered. The criterion for character optimization was DELTRAN (see Gaudin 2004 for justification of this configuration). The analyses consisted of heuristic searches with random addition sequences of 1000 replicas. For reordering of branches, it was selected the TBR algorithm. The topological results of most parsimonious trees were summarized through strict consensus trees.

The methodology of implied weights is intended to mitigate potential biases by limited number of characters (especially osteodermal characters, as consequence of the evolutionary trend in Pampatheriidae towards a simplification of the ornamentation in comparison with that in other cingulate clades, e.g. Glyptodontidae) and the effect of homoplastic characters (Goloboff et al. 2008; Goloboff 2014). Characters were reweighted using the rescaled consistency index (mean value) of the equally-weighted parsimony analysis (see Ausich et al. 2015 and references there for justification of the use of rescaled consistency index for implied-weights parsimony analyses). A default concavity value (k = 3) was selected (Goloboff et al. 2018). Three successive rounds of character reweighting were needed until identical set of strict consensus trees were found in two consecutive searches (Swofford & Bell 2017).

Node support for the strict consensus tree resulting from the equally-weighted analysis was evaluated from absolute Bremer support values, while the node stability for the strict consensus tree obtained from the implied weighting analysis was evaluated using a bootstrap resampling procedure. The software FigTree v1.4.3 (http://tree.bio.ed.ac.uk/software/figtree/) was used as graphical viewer and editor of cladograms.

Taxonomical and nomenclatural criteria

I applied a taxonomical and nomenclatural criterion reasonably, but not strictly, constrained by the phylogeny. This implies looking for a natural classification (i.e. based on monophyletic groups) without ignoring possible limitations of the phylogenetic inference

related to the available information in the fossil record and major morphological gaps. Additionally, it was used open nomenclature to indicate taxonomical uncertainty when necessary, following general recommendations of Bengston (1988) and updated definitions by Sigovini et al. (2016) for the qualifiers of this semantic tool of taxonomy.

Institutional abbreviations

CFM, Museo Nacional de Costa Rica, Colección de fósiles de la sección de Geología, San José, Costa Rica; FMNH, Field Museum Natural History, Chicago, Illinois, USA; Museo Argentino de Ciencias Naturales “Bernardino Rivadavia”, Colección de Paleovertebrados, Ciudad Autónoma de Buenos Aires, Argentina; MLP, Museo de La Plata, La Plata, Argentina; MUN STRI, Museo Mapuka de la Universidad del Norte, Colección de paleontología, Barranquilla, Colombia; UCMP, University of California Museum of Paleontology, Berkeley, California, USA; UF, Florida Museum of Natural History, Gainesville, Florida, USA; VPPLT, Museo de Historia Natural La Tatacoa, Colección de paleontología, La Victoria Town, Huila, Colombia.

Anatomical abbreviations

AM, anterior margin; FL, frontal bone length; GFL, greatest femoral length; GSL, greatest skull length; LCE, longitudinal central elevation; LD, longitudinal depression; LM, lateral margin; LUR, length of the upper teeth row; ME, marginal elevation; Mf, upper molariform; mf, lower molariform; NL, nasal bone length; PAL, parietal bone length; PL,

hard palate length; TTW, maximum width at the third trochanter of the femur; DW, maximum width of the femoral distal epiphysis.

RESULTS

Cladistic analyses

The parsimony analysis with equal weights obtained 107 most parsimonious trees (MPTs), each one of these with a tree length of 44 steps (consistency index = 0.909; retention index = 0.907; rescaled consistency index = 0.825). The strict consensus tree from these MPTs (Fig. 2A; tree length = 52; consistency index = 0.769; retention index = 0.721; rescaled consistency index = 0.555) is not fully resolved because it has two polytomies. One of these polytomies involves the species *S. hondaensis*, *S. antelucanus* and *H. floridanus*, while the other one is formed by *H. septentrionalis*, *H. major*, *H. paulacoutoi* and *H. occidentalis*. Three clades were recovered (excluding that of the entire ingroup): (1) All the ingroup taxa except “Castilletes specimens”; (2) *S. carinatum* + *K. paranensis*; and (3) *Holmesina* spp. except *H. floridanus*. On other hand, the parsimony analysis with implied weights yielded 30 most parsimonious trees (MPTs), each one of those with a tree length of 109 weighted steps (consistency index = 0.982; retention index = 0.982; rescaled consistency index = 0.964). The strict consensus tree from the MPTs (Fig. 2B; tree length = 91; consistency index = 0.978; retention index = 0.980; rescaled consistency index = 0.959), like that produced by the equally weighted approach, is not fully resolved. Again, two polytomies, but in this case the polytomy including *S. hondaensis*, *S. antelucanus* and *H. floridanus* was altered. The latter taxon is placed as the basal-most *Holmesina* species. The polytomy

formed by *H. septentrionalis*, *H. major*, *H. paulacoutoi* and *H. occidentalis* was unmodified. As consequence of the relocation of *H. floridanus* within the topology, four clades were recovered: (1) All the ingroup taxa except "Castilletes specimens"; (2) *S. carinatum* + *K. paranensis*; (3) *Holmesina* spp.; and (4) *H. septentrionalis*, *H. major* + *H. paulacoutoi* + *H. occidentalis*. According to the two schemes of weighting for the parsimony analyses, the genus *Scirrotherium* is paraphyletic if it is composed by *S. antelucanus*, *S. hondaensis* and *S. carinatum*. *S. carinatum* is closer to *K. paranensis* than to *S. hondaensis* or *S. antelucanus*. The relationships among *S. hondaensis* and *S. antelucanus* is not resolved in either of the two strict consensus trees.

In the strict consensus tree from the equally-weighted analysis there is moderate node support for the clade *S. carinatum* + *K. paranensis* (Bremer support value = 3). The clades (1) *Scirrotherium* spp. + *K. paranensis* + *Holmesina* spp.; and (2) *Holmesina* spp. are weakly supported (Bremer support values equal to 1 in both clades). The node stability analysis under implied weights (Fig. 2C) shows high resampling frequencies for the clades (1) *Scirrotherium* spp. + *K. paranensis* + *Holmesina* spp. (bootstrap value = 100); (2) *S. carinatum* + *K. paranensis* (bootstrap value = 100); (3) *Holmesina* spp. (bootstrap value = 99); and (4) *H. septentrionalis* + *H. major* + *H. paulacoutoi* + *H. occidentalis* (bootstrap value = 100). Low resampling frequencies are related to the clades (1) *Scirrotherium* spp. + *K. paranensis* (bootstrap value = 59); and (2) *S. hondaensis* + *S. carinatum* + *K. paranensis* (bootstrap value = 60).

SYSTEMATIC PALAEONTOLOGY

311 XENARTHRA Cope, 1889

312 CINGULATA Illiger, 1811

313 GLYPTODONTOIDEA Gray, 1869

314 Family PAMPATHERIIDAE Paula Couto, 1954

315 Genus *Scirrotherium* Edmund & Theodor, 1997

316 *LSID*. urn:lsid:zoobank.org:act:313358B5-3B1F-4902-8C2E-BB07CFCBEE18

317 *Type species*: *Scirrotherium hondaensis* Edmund & Theodor, 1997 by original designation.

318 *Included species*: In addition to the type species, *S. antelucanus* Laurito & Valerio 2013.

319 *Emended diagnosis*: A pampatheriid of small-to-middle body size that can be distinguished
320 from other pampatheriids by the following combination of features: thin non-marginal fixed
321 osteoderms (~3.5–7 mm in thickness); slightly to moderately rough external surface of
322 osteoderms; external surface of osteoderms with a sharp and uniformly narrow LCE; LCE
323 from superficial to well-elevated; superficial to shallow LDs with gently slope towards the
324 MEs; frequently one single, transversely elongated row of large foramina in the AM of
325 fixed osteoderms; between 6 and 11 anterior foramina as maximum number of foramina per
326 row.

327 *Discussion*: The taxonomical status of *Scirrotherium* is saved from invalidity by paraphyly
328 by exclusion of the species '*S.*' *carinatum* from the genus (see below). However, according
329 to the preferred phylogenetic hypothesis presented here, i.e. the strict consensus tree from
330 the parsimony analysis under implied weights (Fig. 2B), the other two referred species of
331 *Scirrotherium* (*S. antelucanus* and *S. hondaensis*) should be designated in aphyly because

they do not have resolved relationships between them (see Ebach & Williams 2010 for details about the phylogenetic concept of aphyly). Until new evidence available, maintenance of the taxonomical validity of *Scirrotherium*, as defined here, is based on the emended diagnosis of this taxon, which is partially built from ambiguous synapomorphies, as well as from qualitative and quantitative morphological differences with other generic taxa.

Stratigraphic and geographical distribution: [Tentatively, by badly preserved material] Castillo Formation, upper Lower Miocene, upper Burdigalian, Lara State, Venezuela (Rincón et al. 2014); Castilletes Formation, upper Lower to lower Middle Miocene, upper Burdigalian to Langhian; Department of La Guajira, Colombia; La Victoria Formation and Villavieja Formation, upper Middle Miocene, Serravalian, Department of Huila, Colombia (Edmund & Theodor 1997); Caujarao Formation, lower Upper Miocene, Tortonian, Falcon State, Venezuela (Carrillo-Briceño et al. 2018); Curré Formation, Upper Miocene, Puntarenas Province, Costa Rica (Laurito & Valerio 2013); Sincelejo Formation, Upper Miocene to Lower Pliocene, Messinian-Zanclean, Department of Sucre, Colombia; Ware Formation, Upper Pliocene, Piacenzian, Department of La Guajira, Colombia.

Scirrotherium hondaensis Edmund & Theodor, 1997

LSID. urn:lsid:zoobank.org:act:E3B83181-91D6-44C8-90C0-BBAACEC2CDEE

Holotype: UCMP 40201, incomplete skull and left hemimandible.

Type locality and horizon: Municipality of Villavieja, Department of Huila, Colombia. La Victoria Formation, upper Middle Miocene, Serravalian.

354 *Referred material*: VPPLT 004, several fixed osteoderms; VPPLT 264, several fixed
355 osteoderms and one semi-mobile osteoderm; VPPLT 348, tens of fixed and (semi) mobile
356 osteoderms; VPPLT 701, several fixed osteoderms; VPPLT 706, one anterior skull, one
357 femoral diaphysis, one ulna without distal epiphysis, several vertebrae and numerous fixed
358 and (semi) mobile osteoderms; VPPLT 1683 - MT 18, several fixed and (semi) mobile
359 osteoderms; UCMP 39846, one proximal femoral epiphysis, one left calcaneum and one
360 left astragalus. All the osteoderms referred to *S. hondaensis* are illustrated in the Fig. 3.
361 Other important specimens are illustrated in the Figs. 4–7.

362 *Stratigraphic and geographical provenance*: The samples VPPLT 004, 264, 701, 706 and
363 (partially) 1683 - MT 18 were collected in the La Victoria Formation, upper Middle
364 Miocene (Serravalian; see the Figs. 3–6 for more details on the stratigraphic provenance of
365 individual specimens), while the sample UCMP 39846 and part of VPPLT 1683 - MT18
366 comes from the Villavieja Formation, upper Middle Miocene (Serravalian).

367 *Emended differential diagnosis*: Pampatheriid of small body size that differs from other
368 pampatheriids on this unique combination of characters: external surface of osteoderms
369 with ornamentation (especially the LCE and MEs), in general terms, more protuberant than
370 in *S. antelucanus*, but less than in *Kraglievichia*; size range of fixed osteoderms smaller
371 than in *S. antelucanus* and similar to that in *Kraglievichia carinatum* comb. nov. (= '*S.*'
372 *carinatum*; Góis et al. 2013; see below); fixed osteoderms generally thicker than in *K.*
373 *carinatum* comb. nov. but less than in *K. paranensis*, similar to *S. antelucanus*; anterior
374 foramina smaller than in *S. antelucanus*; anterior foramina in fixed osteoderms usually
375 aligned in one individual row, although infrequently these osteoderms show an extra, short
376 or reduced row of anterior foramina; two rows of anterior foramina in mobile osteoderms,

similar to *Vassallia* (Góis 2013); last lower molariform (mf9) incipiently bilobed; frontals prominently convex in lateral view, with this convexity in a posterior position to the insertion of the anterior root of the zygomatic arch; anterior root of the zygomatic arch posterolaterally projected with respect to the main body of maxilla.

Comparative description

For the original and detailed description of this species, including its osteoderms, see Edmund & Theodor (1997). See the Tables 1 and 2 for an updated compilation of osteodermal measurements of referred *Scirrotherium* species and comparisons with those of related taxa. Below there are descriptions of osteological structures and traits incompletely known or unknown for *S. hondaensis* so far.

Skull: The holotype of *S. hondaensis* UCMP 40201 includes a very fragmentary skull. This specimen does not preserve the anterior end of the rostrum, the most of the bone architecture at the orbit level (both dorsally and ventrally), part of the upper dental series, ear region, braincase nor occipital region. Comparatively, the skull of the sample VPPLT 706 (Fig. 4), here originally described, is more complete, despite it also has some missing structures. This new, small skull (see Table 3 for morphometric comparisons) is relatively well preserved from the orbit level to the most anterior end of rostrum, except for the anterior zygomatic arch and nasals dorsally. It also has a less deformed rostrum than that of the holotypic skull of this species. The general aspect of the new skull is similar to those of all known skulls of Pampatheriidae. In lateral view, this is markedly depressed towards its anterior end. In dorsal view, it is tapered also towards its anterior rostrum, where it ends

399 abruptly. Proportionally, the rostrum is shorter than in *K. paranensis* and even more than in
400 *H. floridanus*. In lateral view, the facial process of premaxilla is less defined than in *H.*
401 *floridanus* and the premaxilla-maxilla suture has a convex form, like the former species
402 (Gaudin & Lyon, 2017). The anterorbital fossa is arranged more vertically than in *K.*
403 *paranensis* and *H. floridanus*. The lacrimal is, proportionally, the largest among
404 pampatheriids. This bone severely restricts the frontomaxillary contact in lateral view,
405 similarly to *K. paranensis*. The dorsal contribution of the lacrimal to the orbit is,
406 proportionally, greater than in *H. floridanus* and similar to that in *K. paranensis*. The
407 lacrimal foramen is anteriorly located and close to the anterior border of the orbit. The
408 anterior root of zygomatic arch is projected posterolaterally, unlike other pampatheriids
409 whose skull is known (lateral projection). The frontals show a conspicuous convexity in a
410 posterior position to the insertion of the anterior root of zygomatic arch, in such a way that
411 the posterior section of frontals is placed in a very different plane with respect to that of the
412 anterior section of the same bones. Dorsally, the frontals are more anteroposteriorly
413 elongated and more laterally expanded that in *K. paranensis*, similar to *Holmesina* spp.
414 Ventrally, the hard palate has a wide aspect since the rostrum is shortened in comparison
415 with other pampatheriids. Only two anterior molariforms are preserved (one Mf1 and one
416 Mf2 in different rows) and inferences about upper dentition are made from the alveoli. The
417 upper dental series, as in all the members of the family, is composed by nine molariforms.
418 Of these teeth, the last five (Mf5-Mf9) are bilobed. The anterior molariforms (Mf1-Mf4)
419 converge anteriorly between them, but they do not imbricate. The former teeth are rounded
420 to elliptical, similarly to the condition observed in *H. floridanus*. They also are less
421 mesiodistally elongated than in *K. paranensis*. The molariforms with greatest occlusion
422 area are the fifth and sixth (Mf5 and Mf6). The area of occlusion of the upper molariforms

423 decrease distally from the fifth and sixth molariforms to the ninth, as in all the
424 pampatheriids. The last upper molariform (Mf9) is the smallest of lobed molariforms and
425 has the lesser degree of lobulation (elliptical shape for the material described by Edmund &
426 Theodor 1997). In ventral view, the specimen VPPLT 706 is characterized by a gradual
427 lateral widening of the maxilla from the level of the anterior border of the fifth upper
428 molariform (Mf5). It is preserved the anterior section of palatines as far as a level slightly
429 posterior to the last molariform (Mf9). The maxilla-palatine suture is not recognizable.

430 *Femur:* This bone in *S. hondaensis* was unknown so far, despite the existence of a pair of
431 epiphyses (proximal and distal) from a left femur at the UCMP collections (UCMP 39846).
432 Within the sample VPPLT 706 there is a left femur (Fig. 5A–D) without epiphyses
433 (apparently it is not the same bone from which come the previously referred epiphyses).
434 Thus, the complementary description of all these anatomical elements allows to reconstruct
435 the overall femoral appearance and features. The estimated proximo-distal length of this
436 appendicular bone is ca. 162 mm and its transverse width at third trochanter is 27.6 mm.
437 These morphometric values are the smallest ones for known femora of Pampatheriidae
438 (Table 4). They are only comparable to those of the specimen MLP 69-IX-8-13A which
439 was referred to *K.* cf. *paranensis* (Góis 2013; Scillato-Yané et al. 2013). The femoral head
440 is hemispheric and the greater trochanter is less high than in *K.* cf. *paranensis*, similar to
441 the condition observed in *H. floridanus*. However, the greater trochanter has a more tapered
442 proximal end than in the latter species. In *S. hondaensis*, the lesser trochanter is less
443 mediolaterally expanded than in *K.* cf. *paranensis*. The femoral diaphysis is less curved
444 than in *K.* cf. *paranensis*, similar to that in *H. floridanus*. The border located laterally and
445 distally with respect to the third trochanter is more curved than in *H. floridanus*, similar to

446 that of *K.* cf. *paranensis*. The third trochanter is, proportionally, larger than in *K.* cf.
447 *paranensis*, but less than in *H. floridanus*. The former bone projection is poorly tapered in
448 comparison with the same structure in *P. humboldtii*. The patellar facets are less defined or
449 delimited than in *K.* cf. *paranensis*. In *S. hondaensis* these facets are oriented toward the
450 center of the anterior surface of the distal epiphysis, rather than laterally like in *K.* cf.
451 *paranensis* and *H. floridanus*.

452 *Ulna*: This bone is also described here for the first time. In this case, a right ulna (Fig. 5E–
453 H) without part of the diaphysis and the distal epyphysis. The (incomplete) proximo-distal
454 length is 89.5 mm. The olecranon is elongated and protuberant. In internal view, it is less
455 proximally tapered than in *H. floridanus*. The lateral entrance to the trochlear notch is more
456 restricted than in *Pampatherium*, similarly to *Holmesina*. Likewise, it is less proximo-
457 distally elongated than in *H. floridanus*, more similar to that in *H. paulacoutoi*. Proximally,
458 at the level of the trochlear notch, the posterior border is uniformly convex, not slightly
459 concave, like in *H. floridanus*. The depression for the insertion of the anconeus muscle is
460 deep and more proximally located than in *Pampatherium*, similar to *Holmesina*.

461 *Vertebrae*: Some vertebrae are also reported (Fig. 6). One of these is a thoracic vertebra and
462 five are caudal vertebrae, which four are articulated in two pairs and one is an isolated
463 distal caudal vertebra. The body of the thoracic vertebra is anteriorly eroded, as well as the
464 anterior zygapophyses. Posteriorly, the vertebral body has an outline similar to that of other
465 pampatheriids. The vertebral body is proportionally higher than in *Tonnicintus mirus*.
466 Notably, two ventrolateral apophyses are projected from the vertebral body, like some
467 thoracic vertebrae in *T. mirus* (Góis et al. 2015). Although fragmented, the neural spine of
468 the same vertebra is inferred as proportionally shorter than in *H. floridanus* and *T. mirus*.

469 On other hand, the anterior caudal vertebrae have a posteriorly oriented and tall neural
470 spine. The transverse processes are relatively little extended to the sides.

471 *Astragalus*: In Edmund & Theodor (1997) was mentioned the existence of numerous
472 undetermined postcranial elements whose description was postponed to include it in other
473 publication. However, that description was never published. This postcranial material
474 comprises, within the specimens recovered from the UCMP collections, a left astragalus
475 (UCMP 39846; Fig. 7A–D). In dorsal view, it is observed a lateral trochlea considerably
476 larger than the medial trochlea. The astragalar head is bulging, spherical, almost uniformly
477 convex. There is a shallow concavity in the dorsal margin of the astragalar head whose
478 function has been not determined, but it could be for tendinous insertion and attachment.
479 The astragalar neck is well-differentiated, similar to *Holmesina* and in contrast with that
480 observed in *Pampatherium*. In ventral view, the facets of articulation with the calcaneum,
481 i.e. ectal and sustentacular, are widely separated between them as one would be expect
482 from the observations on their counterparts in the calcaneum (Edmund 1987). According to
483 this, the ectal facet is noticeably larger than the sustentacular facet, unlike *H. floridanus*.
484 The ectal facet is kidney-shaped and the sustentacular facet has a sub-oval shape. Both of
485 them are concave, especially the ectal facet which is very deep. The sustentacular facet is
486 located in a central position within the astragalar neck.

487 *Calcaneum*: This foot bone is other postcranial element not described by Edmund and
488 Theodor for *S. hondaensis*. A well-preserved left calcaneum is associated with the catalog
489 number UCMP 39846 (Fig. 7E–F). This specimen has a proximo-distal length of 54.12 mm
490 and a width at the level of facets (ectal and sustentacular) of ~10.2 mm. These values are
491 the smallest for calcanei referred to Pampatheriidae. The only one species whose known

492 calcaneum is comparable in size to that of *S. hondaensis* is *H. floridanus*. The calcaneum of
493 the latter species is slightly more proximo-distally elongated than in *S. hondaensis*, but it is
494 around twice wider at the level of the ectal and sustentacular facets. This means that the
495 calcaneum of *H. floridanus* is more robust than that of *S. hondaensis*. The calcaneal head is
496 anteroposteriorly elongated, like in *H. floridanus* and unlike the proportionally short
497 calcaneal head of *H. septentrionalis*. The anterior end of the calcaneal head is less truncated
498 that in *Holmesina*. The calcaneum of *S. hondaensis* shows there is no contact between the
499 borders of the ectal and sustentacular facets, similar to species of *Holmesina* other than *H.*
500 *floridanus* and *Pampatherium* (Góis 2013). These facets are slightly convex and they are
501 separated by a moderately deep and very width groove, i.e. the *sulcus tali* (see below). Like
502 *H. floridanus*, the same facets are highly asymmetrical but in *S. hondaensis* this condition is
503 even extreme as the ectal facet is much larger than the sustentacular facet. Additionally, the
504 shape of these facets is disparate between them, i.e. kidney-shaped ectal facet and sub-oval
505 sustentacular facet. The ectal facet is located at an oblique angle with respect to the long
506 axis of the tuber calcanei, unlike *H. floridanus* and similar to *Dasypus*. Like other
507 pampatheriids, the sustentacular facet of the calcaneum of *S. hondaensis* is located
508 anteriorly to the anterior border of the ectal facet. However, this facet is even more
509 anteriorly placed than in other species as consequence of the wide *sulcus tali* that separates
510 the ectal facet with respect to the sustentacular one. Posteriorly, the calcaneal tuber is not
511 massive in comparison with late diverging species of *Holmesina* (e.g. *H. septentrionalis*
512 and *H. paulacoutoi*), but rather it is slender because a mediolateral compression,
513 particularly towards its dorsal side.

514 *Stratigraphic and geographical distribution*: Possibly the Castilletes Formation, upper
515 Lower to lower Middle Miocene, upper Burdigalian to Langhian, Department of La
516 Guajira, Colombia (Fig. 9C); La Victoria and Villavieja Formation, upper Middle Miocene,
517 Serravalian, Department of Huila, Colombia (Edmund & Theodor 1997).

518

519 *Scirrotherium antelucanus* Laurito & Valerio, 2013

520 *LSID*. urn:lsid:zoobank.org:act:225CD304-3B63-4B55-B8B8-33B46C90A194

521 *Holotype*: CFM-2867, mobile osteoderm.

522 *Type locality and horizon*: San Gerardo de Limoncito, Coto Brus county, Puntarenas
523 Province, Costa Rica. Upper Curré Formation, Upper Miocene. For further information
524 about the stratigraphic position of the Curré Formation, see these references: Lowery 1982;
525 Yuan 1984; Rivier 1985; Kolarsky et al. 1995; Alvarado et al. 2009; Aguilar et al. 2010;
526 Obando 2011. There are no absolute ages for this geological unit.

527 *Referred material*: MUN STRI 36880, an isolated fixed osteoderm (Fig. 8).

528 *Stratigraphic and geographical provenance:* Upper Sincelejo Formation, Upper Miocene
529 to Pliocene (Messinian to Zanclean). El Coley Town, Municipality of Los Palmitos,
530 Department of Sucre, Colombia. For further information about the stratigraphic position of
531 the Sincelejo Formation, see these references: Flinch 2003; Villarroel & Clavijo 2005;
532 Bermúdez et al. 2009; and Alfaro & Holz 2014. There are no absolute ages for this
533 geological unit.

534 *Diagnosis*: Unmodified (see Laurito & Valerio, 2013; p. 47).

535 *Comparative description*: The fixed osteoderm of the pelvic shield MUN STRI 36880 is
536 assigned to the species *S. antelucanus* on the basis of the following observations: (I) the
537 area and thickness of this osteoderm (linear measurements in millimetres: anteroposterior
538 length = 34.91; transverse width = 24; thickness = 4.45; approximate area = 837.8 mm^2) are
539 within the range of variability for comparable osteoderms of *S. antelucanus* and exceed the
540 known values of area for most of the same kind of osteoderms for *S. hondaensis*; (II) the
541 external surface is relatively smooth; (III) the AM is wide; (IV) the anterior foramina are
542 larger (2–3 millimetres of diameter) than in *S. hondaensis*, like *S. antelucanus* from Costa
543 Rica; (V) the number of anterior foramina (9) is within the range of variability for *S.*
544 *antelucanus* (7–10 for quadrangular osteoderms, as the specimen here described), greater
545 than in *S. hondaensis*; (VI) poorly elevated LCE, even superficial, like in some osteoderms
546 of *S. antelucanus* (generally LCE more elevated in *S. hondaensis*; see Laurito & Valerio
547 2013).

548 *Stratigraphic and geographical distribution*: Curré Formation, Upper Miocene, Puntarenas
549 Province, Costa Rica (Laurito & Valerio 2013); Sincelejo Formation, Upper Miocene to
550 Lower Pliocene, Messinian to Zanclean, Department of Sucre, Colombia.

551

552 aff. *Scirrotherium*

553 *Referred material*: MUN STRI 16718 (Fig. 9A), fixed osteoderm of the scapular shield;
554 MUN STRI 38064 (Fig. 9E), undetermined fixed osteoderm; MUN STRI 16719 (Fig. 9G),
555 mobile osteoderm fragmented in its AM.

556 *Stratigraphic and geographical provenance*: Castilletes Formation, upper Lower Miocene
557 to lower Middle Miocene, upper Burdigalian to Langhian). Localities of Makaraipao,
558 Kaitamana and Patajau Valley (localities with numbers 390093, 430202 and 390094 in
559 Moreno et al. 2015, respectively), Municipality of Uribia, Department of La Guajira,
560 Colombia.

561 *Comparative description*: The fixed osteoderm of the scapular shield MUN STRI 16718
562 (Fig. 9A) is relatively large and has a pentagonal outline. Its linear measurements in
563 millimetres are: anteroposterior length = 45.02; transverse width = 33.41; thickness = 6.66.
564 These values imply that this osteoderm has greater area than any other known area size for
565 osteoderms referred to *Scirrotherium* (Table 1), including those of the osteoderms of the
566 larger *Scirrotherium* species, i.e. *S. antelucanus* (see Appendix 1 in Laurito & Valerio
567 2013). Rather, this osteoderm size is similar to those reported for *H. floridanus* and *P.*
568 *humboldtii*. The external surface of the osteoderm MUN STRI 16718 is punctuated by
569 numerous diminutive pits, like *S. hondaensis* and *S. antelucanus*. In this surface it is not
570 possible to differentiate a LCE nor LDs, in such a way the osteoderm has a flattened
571 appearance, similar to the case of several osteoderms of *S. antelucanus* (Laurito & Valerio
572 2013). In contrast, the MEs are clearly recognizable. These ridges are relatively low and
573 narrow. There are foramina with a nearly homogeneous large size in the AM. They are
574 aligned in two well defined rows. The most anterior row has five foramina and the posterior
575 to this one has six. Collectively, the two foramina rows are equivalent to ~25% of the
576 anteroposterior length of the osteoderm. In *Scirrotherium*, the foramina rows of fixed
577 osteoderm, when present, this percentage is less than 20%.

MUN STRI 38064 (Fig. 9E): This osteoderm has a trapezoidal outline and the following measurements in millimetres: anteroposterior length = 39.08; transverse width = 39.55; thickness: 5.98. These values are within the range of variability of *S. antelucanus*. This osteoderm has two long rows of anterior foramina of which the posterior row seems to extend partially over the anterior LMs, unlike the anterior foramina row(s) in *S. hondaensis* and *S. antelucanus*. The most anterior foramina row is formed by eight foramina and the posterior to this one has 11 foramina. In both of these rows, foramina have similar size between them, although a few ones are comparatively tiny. The foramina rows diverge on the left LM and within the resultant space is located a large and isolated foramen, i.e. not clearly aligned with any row. This osteoderm does not have recognizable LCE nor LDs, i.e. it is flattened. Its MEs are narrow and poorly elevated. The foramina of LMs are smaller than most of anterior foramina. As consequence of preservation factors, expected pits on the external surface are not present.

MUN STRI 16720 (Fig. 9G): This partial mobile osteoderm has an elongated rectangular shape. Its linear measurements in millimetres are: anteroposterior length (incomplete by fragmentation) = 45.68; transverse width = 30.69; thickness = 6.96. The external surface is convex and without LCE nor LDs. The AM shows an apparently unordered foramina set.

Discussion: With current evidence, the former material should not be confidently assigned to *Scirrotherium* and even less so to create a monospecific genus. This taxonomical decision is supported by several arguments. First, morphologically, the osteoderms here referred to aff. *Scirrotherium* are more similar to those of *S. hondaensis* and *S. antelucanus* than to any other osteoderms of known pampatheriids. The osteoderms of aff. *Scirrotherium* fundamentally differ with respect to the osteoderms of *S. hondaensis* and *S.*

601 *antelucanus* in three characteristics: (I) greater number of anterior foramina and/or greater
602 development of two rows from these foramina; (II) LCE possibly absent, i.e. flattened
603 external surface; (III) larger maximum osteoderm area. Of these features, the third one (III)
604 is the less ambiguous, i.e. the maximum area of fixed osteoderms exceeds those of the
605 osteoderms of *S. hondaensis* and *S. antelucanus*. Comparatively, the first and second (I and
606 II) characteristics are more ambiguous considering that similar conditions were also
607 observed in *S. hondaensis* and *S. antelucanus*. These conditions are described as follows.
608 Some infrequent osteoderms of *S. hondaensis* have two anterior foramina rows, of which
609 the most anterior row is comparatively less developed (i.e. less foramina and smaller) than
610 in aff. *Scirrotherium.* Additionally, in *S. hondaensis* and, particularly in *S. antelucanus*,
611 some osteoderms have flattened and diffuse LCE, even apparently absent. These
612 observations imply limitations on the taxonomical resolution, especially considering that
613 the material on which is based aff. *Scirrotherium* is scarce and it does not allow
614 comparisons from a representative osteoderm series of the morphological variability within
615 the carapace of this animal.

616

617 Genus *Kraglievichia* Castellanos, 1927

618 *LSDI.* urn:lsid:zoobank.org:act:92C8B169-4F79-467E-B951-EF1DE6E327B1

619 *Type species*: *Kraglievichia paranensis* Ameghino, 1883

620 *Included species*: In addition to the type species, *Kraglievichia carinatum* comb. nov.

621 *Emended differential diagnosis*: Small-to-middle sized pampatheriid characterized by fixed
622 osteoderms with ornamentation (particularly the LCE) more conspicuous than in any other

623 pampatheriid; anteriorly wide posteriorly tapered LCE; very deep LDs; highly elevated and
624 frequently blunt MEs, even flattened towards their top; external surface of osteoderms
625 generally rougher than in *Scirrotherium* but less than in *Holmesina*.

626

627 *Kraglievichia carinatum* comb. nov.

628 *Synonyms*: *Scirrotherium carinatum* (Góis et al. 2013).

629 *Holotype*: MLP 69-IX-8-13-AB, a mobile osteoderm.

630 *Type locality and horizon*: Paraná River cliffs, Entre Ríos Province, Argentina. Ituzaingó
631 Formation, Upper Miocene, Tortonian.

632 *Referred material*: In addition to the holotype, the paratypes and part of the hypodigm of
633 this species (see Fig. 10 and Appendix S1 of the Supplementary Material).

634 *Differential diagnosis*: Unmodified (see Góis et al. 2013, p. 182).

635 *Discussion*: In their descriptive work on *K. carinatum* comb. nov., Góis et al. (2013) did
636 not explicitly justify the inclusion of this species within *Scirrotherium*. Interestingly, part of
637 the material assigned to the taxon they create, coming from northwestern Brazil (Solimões
638 Formation), was previously referred to *Kraglievichia* sp. by several researchers, including
639 Góis himself (Góis et al. 2004; Góis 2005; Cozzuol 2006; Latrubesse et al. 2010; Góis et al.
640 2013). However, Góis et al. (2013) refuted the original taxonomical assignment arguing
641 this was erroneous, although they did not offer any concrete support for their decision. In
642 absence of a phylogenetic analysis in Góis et al. (2013), we could assume by default that
643 these authors included to *K. carinatum* comb. nov. within *Scirrotherium* because they

644 considered osteodermal features of this species are at least compatible with the generic
645 diagnosis proposed by Edmund & Theodor (1997). Additionally, based on morphological
646 similarity, Góis and colleagues could have hypothesized closer affinities between *K.*
647 *carinatum* comb. nov. and *S. hondaensis* than those between *K. carinatum* comb. nov. and
648 *K. paranensis*.

649 Let do us analyse in detail each of the osteodermal features of *K. carinatum* comb. nov. in
650 relation to the original diagnosis of *Scirrotherium*. According to Edmund & Theodor
651 (1997), the fixed osteoderms of *Scirrotherium* have a small (not specified) number of large
652 piliferous foramina on the AM. These foramina are well spaced and interconnected
653 between them by a distinct channel. This is observed both in *K. carinatum* comb. nov. and
654 *S. hondaensis*. Likewise, the presence of continuous MEs, posteriorly confluent with the
655 LCE, is a trait also shared by the compared species. Finally, the relative osteoderm size of
656 *K. carinatum* comb. nov. is small among pampatheriids, which is in line with the original
657 diagnosis for *Scirrotherium*.

658 In consequence, the osteodermal features of *K. carinatum* comb. nov. are compatible with
659 those mentioned in the diagnosis for *Scirrotherium* by Edmund & Theodor (1997).
660 However, this does not necessarily imply that the taxonomical allocation of *K. carinatum*
661 comb. nov. in the genus *Scirrotherium* is correct. In fact, there are several reasons to
662 consider this is not reliable. Initially, the diagnosis of Edmund & Theodor (1997) contains
663 only three allegedly diagnostic features on osteoderms, including the relative osteodermal
664 size. Furthermore, and more importantly, these “diagnostic features” do not allow to
665 discriminate between *Scirrotherium* and any other genus of pampatheriids. Indeed, in their
666 analysis, Góis et al. (2013) accept that, for instance, the species *Vassallia minuta* also

667 shares the condition about fixed osteoderms with a small number of large anterior foramina,
668 which are well spaced and connected through a distinguishable canal. Independently,
669 Laurito & Valerio (2013) also highlighted the non-diagnostic nature for *Scirrotherium* of
670 the former osteodermal trait. The other osteodermal features under consideration, i.e. the
671 posterior confluence of the MEs with the LCE and the small osteodermal size, are also
672 ambiguous for positive identification of *Scirrotherium*. For instance, the confluence of MEs
673 and LCE is also found in *K. paranensis*, a pampatheriid clearly different from
674 *Scirrotherium*. And although apparently informative on body-size trends of some individual
675 pampatheriid lineages (e.g. *Holmesina* spp.) and useful as discriminant factor between
676 species (Góis et al. 2013; Laurito & Valerio 2013), the relative osteodermal size is not
677 necessarily insightful in itself to make taxonomical decisions on grouping species in one
678 single genus (see below). In this sense, it is noteworthy the potentially conflictive
679 taxonomical conclusions based predominantly on osteoderm-inferred relative body size in
680 relation with interpretations from non-osteodermal evidence. Thus, for example, the femur
681 MLP 69-IX-8-13A (an adult specimen), which comes from the Ituzaingó Formation and
682 was assigned to *K.* cf. *paranensis* by Scillato-Yané et al. (2013), is comparable in size to
683 that of *S. hondaensis*, i.e. a small pampatheriid. Then, keeping in mind the medium-to-large
684 body size of *K. paranensis*, is probable that the referred femur does not belong to the
685 species *K. paranensis*, although it is reasonable to include it in the genus *Kraglievichia* (as
686 the authors decided). However, Scillato-Yané et al. (2013) did not discuss the possibility
687 that the material assigned to *K.* cf. *paranensis*, particularly the specimen MLP 69-IX-8-
688 13A, has any relationship with the (partially) sympatric species of *K. paranensis*, i.e. *K.*
689 *carinatum* comb. nov., a pampatheriid whose small body size is fully compatible with the
690 small size of that femur. In other words, like Góis et al. (2013), they did not seriously

consider the hypothesis of *K. carinatum* comb. nov. as a small species of *Kraglievichia*, rather than a species belonging to *Scirrotherium*.

Again analysing the original diagnosis for *Scirrotherium* by Edmund & Theodor (1997), it should be regarded as ambiguous and hardly useful to differentiate this genus from other genera in Pampatheriidae, at least with respect to osteodermal traits. Probably these supposedly diagnostic features are actually symplesiomorphies for genera of the family or, at most, a hypothetical subfamilial lineage. This means that Góis et al. (2013) did not have a minimally strong taxonomical background from the original diagnosis of *Scirrotherium* to assign *K. carinatum* comb. nov. to this genus. Alternatively, they may have noticed morphological similarity between osteoderms of *K. carinatum* comb. nov. and *S. hondaensis* from features not included in the diagnosis by Edmund and Theodor. Nevertheless, on their publication, these authors only listed multiple morphological differences between the former species and virtually did not mention any similarity for them, except for potentially equivocal resemblance as that indicated by relative osteodermal size (i.e. small osteodermal sizes in comparison with those of *K. paranensis* and *Plaina*). The lack of usefulness of the relative osteodermal size for generic assignation is further supported by the osteodermal morphometric analysis in Góis et al. (2013, p. 185), whose resulting PCA and CCA plots show that, despite the similarity in relative osteodermal size, *K. carinatum* comb. nov. is located far from *S. hondaensis* (which is closer to *V. minuta*, a taxon apparently related to other main lineage within Pampatheriidae, i.e. *Plaina-Pampatherium*) and *K. paranensis* in morphospace.

Summarizing, there is no solid, possible justification by Góis et al. (2013) on their taxonomical decision to including *K. carinatum* comb. nov. within *Scirrotherium*. The

observation of a common general morphological pattern between *K. carinatum* comb. nov. and *S. hondaensis* does not necessarily imply the grouping of these species under the same generic taxon. Furthermore, we should note that Góis and colleagues, in their work on *K. carinatum* comb. nov., did not make morphological comparisons including to *S. antelucanus*, a species more similar in osteodermal features to *S. hondaensis* (i.e. the type species of *Scirrotherium*). The species *S. antelucanus* was described on a scientific article (Laurito & Valerio 2013) published nearly simultaneously, but later, to that of *K. carinatum* comb. nov. Therefore, Góis et al. (2013) did not know about the existence of *S. antelucanus* when they performed their systematic analysis ("Until the present study, *S. hondaensis* was the only known species of this genus"; Góis et al. 2013, p. 177), so that their taxonomical assignment of *K. carinatum* comb. nov. to *Scirrotherium* was biased by limited notions on the morphological variability and diversity of *Scirrotherium* in northern South America and southern Central America.

In this work I decide to assign *K. carinatum* comb. nov. to the genus *Kraglievichia* based on results of a phylogenetic analysis that I designed considering the hypothesis of Edmund (1985) on the probable subfamilial relationships within Pampatheriidae, which implicitly sustains that the creation of supraspecific taxa from osteodermal evidence should be determined –with the prerequisite of morphological similarity- by the degree of development of the ornamentation. Understanding that *K. carinatum* comb. nov. has morphologically similar osteoderms to those of *K. paranensis* (apart from relative osteoderm size) and has one of the more conspicuous, protuberant osteodermal ornamentations among pampatheriids, along with *K. paranensis*, as acknowledged by Góis et al. (2013) themselves, this means that *K. carinatum* comb. should be considered closely

737 related to *K. paranensis* and therefore they both should also be included in the same genus,
738 i.e. *Kraglievichia*.

739 *Stratigraphic and geographical distribution*: Ituzaingó Formation, Upper Miocene,
740 Tortonian, Entre Ríos Province, Argentina; Puerto Madryn Formation, Upper Miocene,
741 Tortonian, Chubut Province, Argentina; Solimões Formation, Upper Miocene, Tortonian,
742 Acre State, Brazil (Góis et al. 2013).

743

744 **Discussion**

745 This systematic analysis is the first attempt to test the intergeneric relationships and internal
746 structure of the genus *Scirrotherium* with its three previously referred species, i.e. *S.*
747 *hondaensis* (type species), '*S.*' *carinatum* (= *K. carinatum* comb. nov.) and *S. antelucanus*.
748 The two strict consensus trees from the distinct character weighting schemes (equal and
749 implied weights) show very similar results. However, the preferred general phylogenetic
750 hypothesis is that supported by the implied weights analysis. According to Goloboff et al.
751 (2018), the parsimony analysis under implied weights outperforms equal weighting and the
752 model-based methods. This performance inference for the implied weights method is
753 empirically supported here. Beyond this preference for a particular hypothesis (further
754 supported below), both resultant trees agree that all the species referred to *Scirrotherium*
755 are not monophyletic and, consistently, from a diagnostic point of view only *S. hondaensis*
756 and *S. antelucanus* appears as those actually referable to *Scirrotherium*. The relationships
757 between *S. hondaensis* and *S. antelucanus* could not be confidently resolved, despite the
758 inclusion of new osteodermal characters (the only ones comparable between these species

759 so far) in these parsimony analyses. According to the majority-rule consensus tree obtained
760 from the bootstrap resampling, *S. antelucanus* is not the sister taxon of *S. hondaensis*, but it
761 is basal to the clade *S. hondaensis* + '*S*' *carinatum* (= *K. carinatum* comb. nov) + *K.*
762 *paranensis*. However, this clade has low resampling frequency. The basal position of *S.*
763 *antelucanus* within the majority-rule consensus tree is explained to a great extent by a large
764 number of missing entries for *S. antelucanus* in the character matrix. Nevertheless, a non-
765 monophyletic relationship among *S. hondaensis* and *S. antelucanus* should not be rule out.
766 In conjunction, these results suggest the need of information on craniomandibular or dental
767 characters for *S. antelucanus* to test its relationship with respect to *S. hondaensis*. Until new
768 phylogenetic evidence, the genus *Scirrotherium* is maintained as taxonomically valid using
769 a new, emended diagnosis which focus on its lesser degree of development of the
770 osteodermal ornamentation in comparison with those in *Holmesina* and, particularly,
771 *Kraglievichia*. This new diagnosis replaces the original and now inadequate diagnosis of
772 Edmund & Theodor (1997). Composed of *S. hondaensis* and *S. antelucanus*, *Scirrotherium*
773 is considered a coherent taxonomical generic unit according to the criteria of morphological
774 homogeneity and similarity in geographical and chronostratigraphic distributions of its
775 species.

776 Unlike the unpublished phylogeny of Góis (2013), the phylogenetic position of '*S.*'
777 *carinatum* was resolved here, i.e. this species is the sister taxon of *K. paranensis*.
778 Therefore, it is proposed the new name *K. carinatum* comb. nov. Despite Góis (2013) did
779 not recover as a clade to *S. hondaensis* and *K. carinatum* comb. nov., as expected if both
780 these species were assigned to *Scirrotherium*, he presented one supposed synapomorphy
781 that join them, i.e. very deep LDs, "in particular in *S. carinatum*" (Góis 2013, p. 215). This

feature is not a confident support for grouping *S. hondaensis* and *K. carinatum* comb. nov. because the deepest LDs in this main pampatheriid lineage are found in *K. carinatum* comb. nov. and *K. paranensis*, not in *S. hondaensis*. The new emended differential diagnosis for *Kraglievichia* acknowledges the highly sculpted external osteoderm surface documented on this taxon, which is more protuberant than in the Plio-Pleistocene genus *Holmesina*. This diagnosis provides an updated and concise description of useful osteoderm features to distinguish *Kraglievichia* from other genera within Pampatheriidae. It is important to note that the species *K. paranensis* has several autapomorphies (see Appendix S4 of the Supplementary Material) which, in addition to the relative osteoderm size, need to be compared in the future with homologous, unknown (cranial) traits in *K. carinatum* comb. nov. in order to test the phylogenetic closeness of these two species as inferred from osteodermal traits. Provisionally, the difference in relative osteodermal size (consequently also in relative body size) and some morphological differences between *K. carinatum* comb. nov. and *K. paranensis*, as those noted by Góis et al. (2013), may be linked to distinct ontogenetic growth trajectories in these species, being plesiomorphic in nature that of *K. carinatum* comb. nov. (i.e. small body size; see Sánchez-Villagra 2012 for a discussion on the implications for taxonomy of the ontogenetic growth in extinct species). This hypothesis could be extrapolated in some way to the species *S. hondaensis* and *S. antelucanus*.

An important difference here with respect to the phylogeny of Góis is that *K. paranensis* was not recovered as the one single sister taxon of *Holmesina* spp. (except *H. floridanus*). Instead, it is part of a group additionally formed by *S. hondaensis*, *S. antelucanus* and *K. carinatum* comb. nov. Together, these taxa are possibly the sister clade of *Holmesina*. This

means that we do not have evidence of direct ancestral forms to *Holmesina* yet. However, despite some striking differences, it is remarkable the greater morphological similarity between the osteodermal ornamentation and cranial features of *Holmesina* (especially *H. floridanus*) and *Scirrotherium*, rather than with those of *Kraglievichia*. The recognizable similarities between *H. floridanus* and *S. hondaensis*, and at the same time differences with *K. paranensis*, include a less protuberant osteodermal ornamentation; occurrence of uniformly narrower LCE in some osteoderms; more robust skull; more expanded frontals; frontals in a clearly different plane with respect to the parietals; less anteroposteriorly elongated upper teeth; first two upper molariforms less obliquely oriented with respect to the midline of the hard palate; among others.

Apart from that, Góis (2013) found that *Holmesina* is non-monophyletic by the phylogenetic position of *H. floridanus* with respect to the clade groups the other *Holmesina* species. This result coincides with that recovered here from the parsimony analysis with equal weights. The species *H. floridanus* has several plesiomorphic features in comparison with the remaining *Holmesina* species, e.g. less protuberant ornamentation, less rough external surface of the osteoderms and less dorsal basicranium. However, the arrangement of the calcaneal facets of the astragalus in *H. floridanus* (confluent facets) suggests that this species is not directly related to any known South American pampatheriid (Edmund 1987). Likewise, Gaudin & Lyon (2017) have recently found support for the monophyly of *Holmesina* from craniomandibular specimens. Therefore, the position of *H. floridanus* in polytomy with *S. hondaensis* and *S. antelucanus* within the topology of the resultant tree with equal weights is explained from the lack of enough resolution of the analysis (homoplastic noise), not as product of a “real” distant relationship with the remaining

828 *Holmesina* species. Conversely, the genus *Holmesina* is recovered as monophyletic by the
829 implied weights analysis. As expected, in this topology *H. floridanus* is the most basal
830 species of *Holmesina*. In both strict consensus trees, *H. septentrionalis*, the later diverging
831 North American species, is grouped together with all the South American *Holmesina*
832 species (except *H. rondoniensis*, not included in this study).

833 I abstained from revise the diagnosis of the genus *Holmesina* because this is considered
834 beyond the intended objectives of this work. However, six putative synapomorphies
835 (unambiguous and ambiguous) are proposed (or further supported) for this genus: (1)
836 Anterior and lateral margins with elongated, strong bone projections as radii directed from
837 the external border of the central figure towards the osteodermal borders in non-marginal
838 fixed osteoderms; (2) anteriorly convergent, nearly in contact medial processes of
839 premaxillae; (3) length of nasals greater than 30% of the maximum anteroposterior length
840 of the skull; (4) conspicuous and anteroposteriorly elongated maxillary ridge (Gaudin &
841 Lyon 2017); (5) reduced lacrimal; and (6) bilobed posterior upper molariforms (Mf5-Mf9)
842 with incipient trilobulation.

843

844 **Evolutionary and biogeographical implications**

845 *Scirrotherium* is a pampatheriid genus from the Early Miocene-Late Pliocene of northern
846 South America and southern Central America. This taxon, along with *Kraglievichia*,
847 conforms the sister evolutionary line of that gave origin to *Holmesina* (Fig. 12), a
848 pampatheriid probably originated in tropical southern North America (Mexico? see
849 Woodburne 2010). However, based on the osteological comparisons presented above,

which are expanded with respect to those of Edmund (1987), the hypothetical South American ancestor or sister taxon of *Holmesina* probably was morphologically generalized, more similar to *Scirrotherium* or aff. *Scirrotherium* than to *Kraglievichia*. This interpretation is in line with that of Edmund (1987), according to which the calcaneo-astragalar articulation of *S. hondaensis* precludes that this pampatheriid is ancestral to *H. floridanus*, but the ornamentation pattern of the osteoderms suggests "at least some degree of relationship" with the latter species. The genus *Kraglievichia* should be considered a highly, anatomically divergent taxon, especially to taking into account its Miocene age. In Edmund's words, "the osteoderms [of *H. floridanus*] are quite dissimilar to those of *Kraglievichia*" (Edmund 1987, p. 16). This interpretation is partially in conflict with that of Scillato-Yané et al. (2005), according to which *Holmesina* originated from a hypothetical (i.e. not recorded yet) South American basal form of *Holmesina* or *Kraglievichia*. It also is opposed to Simpson (1930) and to the phylogeny of Góis (2013) in which *Kraglievichia* is the sister taxon of *Holmesina*.

The earliest record of *Scirrotherium*, here treated as tentative by scarce and bad-preserved material, comes from the Early Miocene (late Burdigalian) of northwestern Venezuela (Rincón et al. 2014; see below). Independently from the validity of occurrence of *Scirrotherium* in an Early Miocene locality of northern South America, this record represents the oldest pampatheriid reported in the scientific literature so far. This improvement in the fossil record of Pampatheriidae makes it more congruent with the expected time of origination of this family, i.e. Late Oligocene-Early Miocene, according to the very few available time-calibrated phylogenies including representatives of Pampatheriidae and its sister group, i.e. Glyptodontidae (e.g. Fernícola 2008; Billet et al.

873 2011). Apparently, the Early Miocene Venezuelan pampatheriid indicates an origin of these
874 xenartrans in low latitudes in South America. However, this hypothesis could be challenged
875 by a possible Late Eocene pampatheriid of Argentina, which has been not formally
876 described and published yet (Góis 2013).

877 Beyond the geographical origin of Pampatheriidae, northern South America seems to have
878 been a critical area for the early diversification of, at least, a main lineage of pampatheriids,
879 i.e. that including *Scirrotherium*. This genus probably differentiated at least as early as the
880 late Early Miocene-early Middle Miocene (late Burdigalian-Langhian) in northernmost
881 South America. The former evolutionary inference is consistent with the late Early
882 Miocene record referred to *Scirrotherium* from Venezuela (Rincón et al. 2014).

883 Collectively, *Scirrotherium* and *Kraglievichia* occupied a large area in South America
884 during the Neogene (Fig. 13). The geographical range of *Scirrotherium* was more restricted
885 than that of *Kraglievichia*, comprising only tropical low latitudes, instead of a wide
886 latitudinal range, as suggested by Góis et al. (2013). The revaluated distributional pattern of
887 *Scirrotherium* is comparable to that of the glyptodontid *Boreostemma*, which is recorded
888 from the Middle Miocene to the Late Pliocene of Colombia and Venezuela (Carlini et al.
889 2008; Zurita et al. 2016). In contrast, the distributional range of *Kraglievichia* is similar to
890 that of other Miocene xenartran taxa at the generic and specific level which occurred in
891 southern South America and northwestern Brazil, but not in the northern or northwestern
892 end of South America (see Ribeiro et al. 2014).

893 Overall, this evidence indicating biogeographical divergence of northwesternmost South
894 America as an independent faunal province, from the late Early Miocene to Middle
895 Miocene and possibly until the Late Miocene to Pliocene, is consistent with the results of

multiple analyses of the South American terrestrial mammal fossil record for the Neogene (Patterson & Pascual 1968; Cozzuol 2006; Ortiz-Jaureguizar & Cladera 2006; Croft 2007; Carrillo et al. 2015; Rincón et al. 2016; Kerber et al. 2017; Brandoni et al. 2019). Apparently, the existence of one or several strong geographical and/or ecoclimatic barriers (e.g. the Pebas Mega-Wetland System, whose expansion climax coincides with the Middle Miocene) in northern South America would explain that regional endemism pattern (MacFadden 2006; Croft 2007; Salas-Gismondi et al. 2015; Jaramillo et al. 2017). At the same time, the development of a late Early-to-Middle Miocene biogeographical divergence between northwesternmost South America and the rest of this continent may account for the evolutionary (morphological) divergence of the genera *Scirrotherium* and *Kraglievichia*.

In the Late Miocene, without a completely formed PLB (O'dea et al. 2016), *Scirrotherium* expanded its geographical range to southern Central America (Fig. 13), suggesting a hypothetical ephemeral land connection (i.e. land span) or, more likely, overwater dispersal between South America and Central America (maybe via rafting mechanism; efficient active swimming of a pampatheriid in a marine channel seems highly improbable). This is the earliest dispersal event of a pampatheriid to North America (see below). The Central American species of *Scirrotherium*, *S. antelucanus*, is larger than *S. hondaensis*, but comparable or even smaller than aff. *Scirrotherium*. From available evidence, it is not possible to determinate the most probable area of evolutionary differentiation of *S. antelucanus*, but now there is support for occurrence of this species in the late Neogene of northwestern South America, specifically in the Department of Sucre, Colombia.

The South American record of *S. antelucanus* is probably several million years younger (3–5 my) than the Central American record. However, given the lack of absolute dating for the fossil-bearing stratigraphic levels and the occurrence of Late Miocene strata in the same geological unit (Sincelejo Formation) where comes the material here assigned to *S. antelucanus* in Colombia, it should be recognized a significant age uncertainty for the new South American record of this species. In any case, this age is considered may be Early Pliocene or, alternatively, Latest Miocene from the stratigraphic position of the fossil-bearing horizons (Villarroel & Clavijo, 2005; Bermúdez et al. 2009; Alfaro & Holz 2014; Bernal-Olaya et al. 2015; Córtes et al. 2018), as well as from associated palynomorphs (Silva et al. 2012; B. Fernandes & C. Jaramillo, pers. comm. 2014).

The biogeographical correlation across the Isthmus of Panama using *S. antelucanus* has insightful implications for the understanding of the late Cenozoic intercontinental migratory dynamics in the Americas, including the Great American Biotic Interchange (GABI) (Webb 2006; Woodburne et al. 2006; Woodburne 2010; Cione et al. 2015; Bloch et al. 2016). Noteworthy, this is the first transisthmian biogeographical correlation for a Neogene terrestrial mammal at the level of species; furthermore, it is the first short-distance intercontinental correlation (i.e. adjacent to the Central American Seaway) with high taxonomical resolution for Neogene land mammals of the Americas; and, finally, it constitutes the first evidence of a distributional pattern congruent with a re-entry event to South America by a pre-Pleistocene xenartran.

We subsequently analyse in more detail these implications. So far, we know a few biogeographical correlations across the Isthmus of Panama which are based on records at generic level of Neogene and Pleistocene land mammals, as well as a very few records at

941 species level of the latter epoch. The Neogene biogeographical correlations include the
942 pampatheriid genera *Plaina*, in Mexico and central-southwestern South America;
943 *Pampatherium*, in Mexico and southeastern South America; and *Holmesina*, in United
944 States, Mexico and El Salvador, as well as in northwestern and southeastern South America
945 (Woodburne 2010). At the level of species, for instance, the Pleistocene megatheriine
946 *Eremotherium laurillardi* has occurrence in both sides of the Isthmus of Panama in North-
947 and South America (Cartelle & De Iuliis 1995, 2006; Tito 2008; McDonald & Lundelius,
948 E. L. Jr. 2009; Martinelli et al. 2012; Cartelle et al. 2015).

949 The record in South America of *S. antelucanus* increase the taxonomical resolution of
950 transisthmian biogeographical correlations of Neogene land mammals, opening the
951 possibility of new correlations of this kind and their biostratigraphic application in circum-
952 Caribbean basins, in a similar way as envisioned by the renowned American
953 palaeontologist Ruben A. Stirton from his revision of the fossil mammal remains of "La
954 Peñata fauna" (Stirton 1953), the vertebrate fossil association where comes the new record
955 of *S. antelucanus*. This translates into direct correlation of Land Mammal Ages (in this
956 case, SALMA and NALMA) from migrant mammals which are shared at species level by
957 both South and North America. Using to *S. antelucanus*, this would mean exists a support
958 for faunal, not necessarily chronological, correlation of the early Hemphillian and
959 Montehermosan mammal (xenartran) assemblages in North America and South America,
960 respectively (see Laurito & Valerio, 2013). Nevertheless, naturally, any solid
961 intercontinental faunal correlation implies more than only one taxonomical element for
962 support. The direct intercontinental faunal correlations from Cenozoic land mammals
963 between South and North America are still underdeveloped in comparison with those

964 between other continents (e.g. North America and Europe or North America and Asia;
965 Woodburne & Swisher, C. C. III 1995; Beard & Dawson 1999; Bowen et al. 2002)

966 Additionally, the transisthmian correlation of *S. antelucanus* allows to increase the
967 geographical resolution in detection of intercontinental migrations of late Cenozoic land
968 mammals, which are restricted mainly to large and middle distance correlations for the
969 Neogene record (e.g. Mexico-southern South America; Woodburne 2010). This pattern has
970 prevented the exploration of possible early or intermediate phases of
971 anagenetic/cladogenetic events in late Cenozoic Interamerican migrant taxa, which in turn
972 it is reflected in the fact that we are detecting "suddenly" well-differentiated terminal taxa
973 (e.g. *Holmesina*) in marginal, distant areas with respect to the Central American Seaway
974 and adjacent terrains (Cione et al. 2015 and references therein).

975 On other hand, the new transisthmian correlation here presented suggests a possible
976 Neogene re-entry event by a xenartran to South America after its evolutionary
977 differentiation in North America (Fig. 13). The confirmation of this depends on a confident
978 determination of the differentiation area for *S. antelucanus*, i.e. if this species originated in
979 South America, the new record is explained more parsimoniously by population
980 maintenance in the ancestral area. Conversely, if this species originated in Central America
981 from a South American species of *Scirrotherium* as *S. hondaensis*, then we are considering
982 a re-entry event to South America. However, as mentioned above, it is not possible to
983 constrain much more than that at this moment. In any case, the possibility of a Neogene re-
984 entry event to South America by a xenartran is compatible with the fact that we know
985 several of these events during the Pleistocene. Among these Pleistocene events, there are
986 several involving xenartrans, including the pampatheriids *Holmesina* and *Pampatherium*,

the glyptodontid *Glyptotherium*, the pachyarmatheriid *Pachyarmatherium*, the dasypodid *Dasypus* and the megatheriine *Eremotherium* (Woodburne et al. 2006; Woodburne 2010 and references therein).

Now let's discuss the evolutionary implications of this systematic analysis for the genus *Holmesina* and the multiple Interamerican dispersal events of pampatheriids, including that of *Scirrotherium* (discounting the non-confirmed re-entry event to South America). The genus *Holmesina* has its oldest record (*Holmesina* sp.) in sedimentary rocks deposited around the Pliocene-Pleistocene boundary (~2.4 mya) in La Florida, United States (Edmund 1987; Woodburne 2010 and references there; Gaudin & Lyon 2017). This northward dispersal event is part of the earliest phase of the GABI (GABI 1), in which additionally participated other xenartrans as *Dasypus*, *Pachyarmatherium* and *Eremotherium* (Woodburne 2010). Typically, *H. floridanus* has been considered the most basal among the *Holmesina* species (Edmund 1987), as it is supported here. The time-calibrated phylogeny introduced in this work for Pampatheriidae (Fig. 12) suggests that exist a long ghost lineage leading to *Holmesina*, from the Early Miocene (Burdigalian) until the Late Pliocene. The improvement of the fossil record in northern South America, Central America and Mexico will allow to advance in the recognition of probable direct ancestral forms for *Holmesina*.

From the above analysis, a probable model of biogeographical evolution of *Holmesina* is as follows (Fig. 13). A hypothetical pampatheriid close to *Holmesina* or even a hypothetical *Holmesina* species basal with respect to *H. floridanus* dispersed to Central America, Mexico and United States during the Pliocene (Early Pliocene according the time-calibrated phylogeny). Once it was established the genus *Holmesina* in North America with *H.*

floridanus, the larger species *H. septentrionalis* diverged and differentiated in the Early Pleistocene of southern United States. Later, *H. septentrionalis* expanded southward to Mexico and Central America during the Early-Middle Pleistocene (Aguilar & Laurito 2009). In the Middle or early Late Pleistocene, possibly *H. septentrionalis* colonized South America, where took place an important diversification, which was likely influenced by the Late Pleistocene climatic changes (Scillato-Yané et al. 2005). This diversification gave origin to the species *H. occidentalis*, *H. rondoniensis*, *H. major* and to the most robust pampatheriid, *H.paulacoutoi* (Scillato-Yané et al. 2005).

As inferred from the phylogeny and derived interpretations here presented, the dispersal events of *S. antelucanus* and *H. floridanus* to North America are independent of each other. This means that the number of northward intercontinental dispersal events of pampatheriids during the late Cenozoic actually is at least three, which in chronological order are: (1) genus *Scirrotherium* (Late Miocene); (2) lineage *Plaina-Pampatherium* (Early Pliocene); (3) genus *Holmesina* (undetermined Pliocene). From these events, only the latter, based on the fossil record of *H. floridanus*, is included in the GABI. The remaining two events are classified as part of the macroevolutionary invasion “wastebasket” called “Pre-GABI” (literally, ‘before the GABI’; Woodburne et al. 2006; Woodburne 2010; also named by Cione et al. 2015 as “ProtoGABI”). In the lineage *Plaina-Pampatherium*, it was differentiated one genus, *Pampatherium*, and at least three species (*P. mexicanum*, *P. typum* and *P. humboldtii*, being the two latter recorded in South America). Meanwhile, the northward dispersal event of *Scirrotherium* seems to give no origin to any other species different to *S. antelucanus*. Only a confirmed southward intercontinental dispersal event of the *Scirrotherium-Kraglievichia-Holmesina* clade has been well-established, i.e. that of

1033 *Holmesina* to South America in the Middle or early Late Pleistocene (Aguilar & Laurito
1034 2009). This event probably is not part of any of the GABI phases of Woodburne (2010) but
1035 it is chronologically located between the GABI 2 and 3.

1036 As it has been shown, the study of more abundant and complete pampatheriid material
1037 preserved in Neogene geological units of northern South America, in particular, and the
1038 current intertropical region of the Americas, in general, has the potential of provide us more
1039 complex and interesting scenarios on the evolution of this glyptodontoid family and,
1040 specifically, the genera *Scirrotherium* and *Holmesina*.

1041

1042 **CONCLUSION**

1043 The monophyly of *Scirrotherium* has been tested through parsimony phylogenetic analyses.
1044 This taxon is recovered as paraphyletic if we include all the referred species, i.e. *S.*
1045 *hondaensis, S. antelucanus* and '*S.*' *carinatum*. The latter species is closer to *Kraglievichia*
1046 *paranensis* and, therefore, here it is proposed the new name *K. carinatum* comb. nov. The
1047 remaining referred species to *Scirrotherium, S. hondaensis* and *S. antelucanus*, are designed
1048 in aphyly. The taxonomic validity of *Scirrotherium*, as defined here, is maintained from
1049 diagnostic evidence. The genus *Scirrotherium* is probably the sister taxon of *Kraglievichia*,
1050 and these two genera form the sister clade of *Holmesina*. The genus *Scirrotherium* has
1051 occurrence from the late Early Miocene to Late Pliocene of northwestern South America
1052 (Colombia, Venezuela and northern Peru) and the Late Miocene of southern Central
1053 America (Costa Rica). A geographical origin of Pampatheriidae in northernmost South
1054 America is suggested from the fossil record of *Scirrotherium* and a new time-calibrated

phylogeny. The genus *Scirrotherium* also represents the earliest member of Pampatheriidae which participated in a dispersal event to North America, specifically to the ancient Central American peninsula. This dispersal event happened when the PLB was not fully formed yet. The species *S. antelucanus* lived in Central America and now also in northern Colombia during the late Neogene. This is the first Interamerican biogeographical correlation of a Neogene land mammal with high taxonomical resolution, i.e. at the species level. The record of *S. antelucanus* in both sides of the ancient Central American Seaway is compatible with a possible re-entry event of this pampatheriid to South America. In addition, *Scirrotherium* is not probably the South American ancestor of the originally-endemic North American genus *Holmesina*. In contrast with a previous hypothesis which argues that *Holmesina* may have evolved from *Kraglievichia*, here it is suggested that there is no evidence of direct ancestral forms of *Holmesina*, although the unknown South American ancestor of *Holmesina* may be morphologically more similar to *Scirrotherium.*

Acknowledgements

I am greatly indebted to all curators and managers of the collections visited for revision of specimens during this work, especially to: Andrés Vanegas (Museo de Historia Natural La Tatacoa), Aldo Rincón (Museo Mapuka, Universidad del Norte), Jorge Moreno-Bernal (Museo Mapuka, Universidad del Norte), Carlos De Gracia (Museo Mapuka, Universidad del Norte), Richard C. Hulbert Jr. (Florida Museum of Natural History), Kenneth Angielczyk (Field Museum of Natural History), Bill Simpson (Field Museum of Natural History, Patricia Holroyd (University of California Museum of Paleontology) and Marcelo Reguero (Museo de La Plata). I am also grateful to Carlos Jaramillo (Smithsonian Tropical

1078 Research Institute) and his field work team from allowing access to fossils they collected in
1079 the Deparment of La Guajira (Colombia). Likewise, special thanks to the professor Antonio
1080 Tovar (University of Sucre) by inspiration to explore the Sincelejo Formation; to my field
1081 assistants during this exploration in the Department of Sucre (Colombia), Oscar Melendrez,
1082 Angel Cruz and Juan Pacheco. I would like to thank professor César Laurito (Instituto
1083 Nacional de Aprendizaje de Costa Rica) and Edwin Cadena (Universidad del Rosario) for
1084 providing photos of osteoderms of the species *S. antelucanus* and one photo of outcrops of
1085 the Castilletes Formation, respectively. This work would not have been possible without
1086 logistic support and encourage by Alba Lara, Carolay Jiménez and Mónica Montalvo. An
1087 anonymous reviewer provided comments that made it possible to improve the manuscript.
1088 Financial assistance for this project was provided by several institutions/agencies:
1089 CONICET (Internal Doctoral Fellowship); Field Museum of Natural History (Science
1090 Visiting Scholarship); Florida Museum of Natural History (International Travel Grant);
1091 University of California Museum of Paleontology (Welles Fund); and The Paleontological
1092 Society (PalSIRP-Sepkoski Grant).

1093

1094 DATA ARCHIVING STATEMENT

1095 Data for this study are avalaible in the Dryad Digital Repository: [Intentionally blank]

1096 The nomenclatural acts contained in this work are registered in ZooBank:

1097 *LSID*. urn:lsid:zoobank.org:act:313358B5-3B1F-4902-8C2E-BB07CFCBEE18

1098 *LSID*. urn:lsid:zoobank.org:act:E3B83181-91D6-44C8-90C0-BBAACEC2CDEE

1099 *LSID*. urn:lsid:zoobank.org:act:225CD304-3B63-4B55-B8B8-33B46C90A194

LSID. urn:lsid:zoobank.org:act:92C8B169-4F79-467E-B951-EF1DE6E327B1

REFERENCES

AGUILAR, D. H. and LAURITO, C. A. 2009. El armadillo gigante (Mammalia, Xenarthra, Pampatheriidae) del río Tomayate, Blancano tardío-Irvingtoniano temprano, El Salvador, América Central. *Revista Geológica de América Central*, **41**, 25–36.

AGUILAR, T., ACEVEDO, B. and ULLOA, A. 2010. Paleontología de una sección del río Corredores, Formación Curré, Mioceno, Costa Rica. *Revista Geológica de América Central*, **42**: 43–75.

ALFARO, E. and HOLZ, M. 2014. Review of the chronostratigraphic charts in the Sinú-San Jacinto Basin based on new seismic stratigraphic interpretations. *Journal of South American Earth Sciences*, **56**, 139–169.

ALVARO, G. E., BARQUERO, R., TAYLOR, W., LÓPEZ, A. CERDAS, A. and MURILLO, J. 2009. Geología de la hoja general, Costa Rica. *Revista Geológica de América Central*, **40**: 97–107.

AMEGHINO, F. 1888. Lista de las especies de mamíferos fósiles del Mioceno superior de Monte Hermoso hasta ahora conocidas. Obras Completas y Correspondencia Científica, 5, 481–496.

ANDERSON, V. J., HORTON, B. K., SAYLOR, J. E., MORA, A., TESÓN, E., BREECKER, D. O. and KETCHAM, R. A. 2016. Andean topographic growth and

basement uplift in southern Colombia: Implications for the evolution of the Magdalena, Orinoco, and Amazon river systems. *Geosphere*, **12** (4), 1235–1256.

ANTOINE, P. O., ABELLO, M. A., ADNET, S., SIERRA, A. J., BABY, P., BILLET, G., BOIVIN, M., CALDERON, Y., CANDELA, M. A., CHABAIN, J., CORFU, F., CROFT, D. D., GANERØD, M., JARAMILLO, C., KLAUS, S., MARIVAUX, L., NAVARRETE, R. E., ORLIAC, M. J. and PARRA, F. 2016. A 60-million-year Cenozoic history of western Amazonian ecosystems in Contamana, eastern Peru. *Gondwana Research*, **31**, 30–59.

AUSICH, W. I., KAMMER, T. W., RHENBERG, E. C. and WRIGHT, D. F. 2015. Early phylogeny of crinoids within the pelmatozoan clade. *Palaeontology*, **58** (6): 937–952.

BEARD, K. C. and DAWSON, M. R. 1999. Intercontinental dispersal of Holarctic land mammals near the Paleocene/Eocene boundary; paleogeographical, paleoclimatic and biostratigraphic implications. *Bulletin de la Société géologique de France*, **170** (5), 697–706.

BENGTSON, P. 1988. Open nomenclature. *Palaeontology*, **31** (1), 223–227.

BERMÚDEZ, H. D., ALVARÁN, M., GRAJALES, J. A., RESTREPO, L. C., ROSERO, J. S., GUZMÁN, C., RUÍZ, E. C., NAVARRETE, R. E., JARAMILLO, C. and OSORNO, J. F., 2009. Estratigrafía y evolución geológica de la secuencia sedimentaria del Cinturón Plegado de San Jacinto. *Memorias XII Congreso Colombiano de Geología*, pp. 1–27.

BERNAL-OLAYA, R., MANN, P. and VARGAS, C. A. 2015. Earthquake, tomographic, seismic reflection, and gravity evidence for a shallowly dipping subduction zone beneath

1142 the Caribbean Margin of Northwestern Colombia. *In* BARTOLINI, C. and MANN, P.
1143 (eds.) *Petroleum Geology and Potential of the Colombian Caribbean Margin*. *AAPG*
1144 *Memoir*, **118**, 247–270.

1145 BILLET, G., HAUTIER, L., DE MUIZON, C. and VALENTIN, X. 2011. Oldest cingulate
1146 skulls provide congruence between morphological and molecular scenarios of armadillo
1147 evolution. *Proceedings of the Royal Society of London B, Biological Sciences*, **278**,
1148 2791–2797.

1149 BLOCH, J. I., WOODRUFF, E. D., WOOD, A. R., RINCON, A. F., HARRINGTON, A.
1150 R., MORGAN, G. S., FOSTER, D. A., MONTES, C., JARAMILLO, C. A., JUD, N. A.,
1151 JONES, D. S. and MACFADDEN, B. J. 2016. First North American fossil monkey and
1152 early Miocene tropical biotic interchange. *Nature*, **533** (7602), 243–258.

1153 BOWEN, G. J., CLYDE, W. C., KOCH, P. L., TING, S., ALROY, J., TSUBAMOTO, T.,
1154 WANG, Y. and WANG, Y. 2002. Mammalian dispersal at the Paleocene/Eocene
1155 boundary. *Science*, **295** (5562), 2062–2065.

1156 BRANDONI, D., RUIZ, L. G. and BUCHER, J. 2019. Evolutive Implications of
1157 *Megathericulus patagonicus* (Xenarthra, Megatheriinae) from the Miocene of Patagonia
1158 Argentina. *Journal of Mammalian Evolution*, 1–16.

1159 CARLINI, A. A., ZURITA, A. E., SCILLATO-YANÉ, G. J., SÁNCHEZ, R. and
1160 AGUILERA, O. A. 2008. New Glyptodont from the Codore Formation (Pliocene),
1161 Falcón State, Venezuela, its relationship with the *Asterostemma* problem, and the
1162 paleobiogeography of the Glyptodontinae. *Paläontologische Zeitschrift*, **82** (2), 139–
1163 152.

1164 CARRILLO, J. D., FORASIEPI, A., JARAMILLO, C. and SÁNCHEZ-VILLAGRA, M. R.
1165 2015. Neotropical mammal diversity and the Great American Biotic Interchange: spatial
1166 and temporal variation in South America's fossil record. *Frontiers in Genetics,* **5**, 451,
1167 1–11

1168 CARRILLO-BRICEÑO, J. D., REYES-CESPEDES, A. E., SALAS-GISMONDI, R. and
1169 SÁNCHEZ, R. 2018. A new vertebrate continental assemblage from the Tortonian of
1170 Venezuela. *Swiss Journal of Palaeontology*, 1–12.

1171 CARTELLE, C. and BOHÓRQUEZ, G.A. 1985. *Pampatherium paulacoutoi*, uma nova
1172 espécie de tatu gigante da Bahia, Brasil (Edentata, Dasypodidae). *Revista Brasileira de*
1173 *Zoologia*, **2**: 229-254.

1174 — and DE IULIIS, G. 1995. *Eremotherium laurillardi*: The Panamerican late Pleistocene
1175 megatheriid sloth. *Journal of Vertebrate Paleontology*, **15** (4), 830–841.

1176 — — 2006. *Eremotherium laurillardi* (Lund) (Xenarthra, Megatheriidae), the Panamerican
1177 giant ground sloth: Taxonomic aspects of the ontogeny of skull and dentition. *Journal of*
1178 *Systematic Palaeontology*, **4** (2), 199–209.

1179 — — and PUJOS, F. 2015. *Eremotherium laurillardi* (Lund, 1842) (Xenarthra,
1180 Megatheriinae) is the only valid megatheriine sloth species in the Pleistocene of
1181 intertropical Brazil: A response to Faure et al., 2014. *Comptes Rendus Palevol*, **14** (1),
1182 15–23.

1183 CASTELLANOS, A. 1937. Anotaciones sobre la línea filogenética de clamiterios. *Serie*
1184 *Técnico-Científica de la Facultad de Ciencias Matemáticas, Físico-Químicas y*
1185 *Naturales*, **8**:1–35. Rosario, Argentina.

1186 CIONE, A., GASPARINI, G., SOIBELZON, E., SOIBELZON, L. and TONNI, E. 2015.
1187 *The Great American Biotic Interchange. A South American perspective*. Springer Briefs
1188 in Earth System Sciences. South America and the Southern Hemisphere, Amsterdam,
1189 Netherlands, 97 pp.

1190 COATES, A. G. and STALLARD, R. F. 2013. How old is the Isthmus of Panama? *Bulletin*
1191 *of Marine Science*, **89** (4), 801–813.

1192 CORTES, J. E., AGUILERA, R., WILCHES, O., OSORNO, J. F. and CORTES, S. I. 2018.
1193 Organic geochemical insights from oil seeps, tars, rocks, and mud volcanoes on the
1194 petroleum systems of the Sinú-San Jacinto basin, Northwestern Colombia. *Journal of*
1195 *South American Earth Sciences*, **86**, 318–341.

1196 COZZUOL, M. A., 2006. The Acre vertebrate fauna: age, diversity, and geography.
1197 *Journal of South American Earth Sciences*, **21**, 185–203.

1198 CROFT, D. A. 2007. The Middle Miocene (Laventan) Quebrada Honda fauna, southern
1199 Bolivia and a description of its notoungulates. *Palaeontology*, **50** (1), 277–303.

1200 DE IULIIS, G. and EDMUND, A. G. 2002. *Vassallia maxima* Castellanos, 1946
1201 (Mammalia: Xenarthra: Pampatheriidae), from Puerta del Corral Quemado (late
1202 Miocene to early Pliocene), Catamarca Province, Argentina. *Smithsonian Contributions*
1203 *to Paleobiology*, **93**, 49–64.

1204 DELSUC, F., SUPERINA, M., TILAK, M. K., DOUZERY, E. J. and HASSANIN, A.
1205 2012. Molecular phylogenetics unveils the ancient evolutionary origins of the enigmatic
1206 fairy armadillos. *Molecular Phylogenetics and Evolution*, **62**, 673–680.

1207 EBACH, M. C. and Williams, D. M. 2010. Aphyly: a systematic designation for a
1208 taxonomic problem. *Evolutionary biology*, **37** (2-3), 123–127.

1209 EDMUND, A. G. 1985. The Armor of fossil giant Armadillos (Pampatheriidae,
1210 Xenarthra, Mammalia). Texas Memorial Museum, *Pearce-Sellards-Series*, **40**, 1–20.

1211 **—** 1987. Evolution of the Genus *Holmesina* (Pampatheriidae, Mammalia) in Florida, with
1212 Remarks on Taxonomy and Distribution. Texas Memorial Museum, *Pearce-Sellards-*
1213 *Series*, **45**, 1–20.

1214 **—** and THEODOR, J. 1997. A new giant Armadillo. *In* KAY, R. F., CIFELLI, R. L.,
1215 FLYNN, J. J., and MADDEN, R. (eds.), *Vertebrate Paleontology of the Miocene Fauna*
1216 *of La Venta, Colombia*. Smithsonian Institution Press, Washington, pp. 227–232

1217 FERNÍCOLA, J. C. 2008. Nuevos aportes para la sistemática de los Glyptodontia
1218 Ameghino 1889 (Mammalia, Xenarthra, Cingulata). *Ameghiniana*, **45** (3), 553–574.

1219 FLINCH, J. F. 2003. Structural evolution of the Sinú-Lower Magdalena area (northern
1220 Colombia). *In* BARTOLINI, C., BUFFLER, R. T. and BLICKWEDE, J. (eds.), *The*
1221 *Circum-Gulf of Mexico and the Caribbean: Hydrocarbon Habitats, Basin Formation,*
1222 *and Plate Tectonics*, *AAPG Memoir*, **79**, 776–796.

1223 FLYNN J. J., GUERRERO J. and SWISHER, C. C. III. 1997. Geochronology of the Honda
1224 Group. *In* KAY, R. F., CIFELLI, R. L., FLYNN, J. J., and MADDEN, R. (eds.),

Vertebrate Paleontology of the Miocene Fauna of La Venta, Colombia. Smithsonian Institution Press, Washington, pp. 44–59.

GAUDIN, T. J. 2004. Phylogenetic relationships among sloths (Mammalia, Xenarthra, Tardigrada): the craniodental evidence. *Zoological Journal of the Linnean Society*, **140**, 255–305.

— and WIBLE, J. R. 2006. The phylogeny of living and extinct armadillos (Mammalia, Xenarthra, Cingulata): a craniodental analysis. *In* CARRANO, M. T., GAUDIN, T. J., BLOB, R. W. and WIBLE, J. R. (eds.), *Amniote Paleobiology: Perspectives on the Evolution of Mammals, Birds and Reptiles*, University of Chicago Press, Chicago, pp. 153–198.

— and LYON, L. M. 2017. Cranial osteology of the pampathere *Holmesina floridanus* (Xenarthra: Cingulata; Blancan NALMA), including a description of an isolated petrosal bone. *PeerJ*, **5**, e4022.

GÓIS, F. 2005. Estudo descritivo e geométrico dos Cingulata (Mammalia, Xenarthra) do Neógeno e Quaternário da Amazônia Sul-Ocidental. Unpublished bachelor thesis, Universidade Federal de Rondônia, 58 pp.

— 2013. Análisis morfológico y afinidades de los Pampatheriidae (Mammalia, Xenarthra). Unpublished PhD thesis, Universidad Nacional de La Plata, La Plata, Argentina, 330 pp.

— SCILLATO-YANÉ, G. J., CARLINI, A. A. and UBILLA, M. 2012. Una nueva especie de *Holmesina* Simpson (Xenarthra, Cingulata, Pampatheriidae) del Pleistoceno de Rondônia, sudoeste de la amazonia, Brasil. *Revista Brasileira de Paleontologia*, **15** (2), 211–227.

— SCILLATO-YANÉ, G. J., CARLINI, A. A. and GUILHERME, E. 2013. A new species of *Scirrotherium* Edmund & Theodor, 1997 (Xenarthra, Cingulata, Pampatheriidae) from the late Miocene of South America. *Alcheringa: An Australasian Journal of Palaeontology*, **37** (2), 177–188.

— RUIZ, L. R., SCILLATO-YANÉ, G. J. and SOIBELZON, E. 2015. A peculiar new Pampatheriidae (Mammalia: Xenarthra: Cingulata) from the Pleistocene of Argentina and comments on Pampatheriidae diversity. *PloS One*, **10** (6), e0128296.

— NASCIMENTO, E. R., PORTO, A. S., HOLANDA, E. C. and COZZUOL, M. A. 2004. Ocorrências de Cingulata dos gêneros *Kraglievichia* e *Holmesina* do Terciário e Quaternário da Amazônia Sul-Ocidental. *Ameghiniana*, **49**, 41.

GUERRERO, J. 1997. Stratigraphy and sedimentary environments of the Honda Group in the La Venta area. Miocene uplift of the Colombian Andes. *In* KAY, R. F., CIFELLI, R. L., FLYNN, J. J., and MADDEN, R. (eds.), *Vertebrate Paleontology of the Miocene Fauna of La Venta, Colombia*. Smithsonian Institution Press, Washington, pp. 15–43.

GOLOBOFF, P. A. 2014. Extended implied weighting. *Cladistics*, **30** (3): 260–272.

— TORRES, A. & ARIAS, J. S. 2018. Weighted parsimony outperforms other methods of phylogenetic inference under models appropriate for morphology. *Cladistics*, **34** (4): 407–437.

— CARPENTER, J. M., SALVADOR ARIAS, J. and MIRANDA ESQUIVEL, D. R. 2008. Weighting against homoplasy improves phylogenetic analysis of morphological data sets. *Cladistics*, **24** (5): 758–773.

HOFFSTETTER, R. 1952. Les mammifères pleistocenes de la République de l'Équateur. *Mémoires Societé Géologique de France*, **66**: 1–391.

JARAMILLO, C. 2018. Evolution of the Isthmus of Panama: biological, paleoceanographic, and paleoclimatological implications. *In* HOORN, C. and ANTONELLI, A. (eds.), *Mountains, climate and biodiversity*. John Wiley & Sons, Oxford, pp. 323–338

— ROMERO, I., D'APOLITO, C., BAYONA, G., DUARTE, E., LOUWYE, S., ESCOBAR, J., LUQUE, J., CARRILLO-BRICEÑO, J. D., ZAPATA, V., MORA, A., SCHOUTEN, S., ZAVADA, M., HARRINGTON, G. and WESSELING, F. P. 2017. Miocene flooding events of western Amazonia. *Science advances*, **3** (5), e1601693.

KERBER, L., NEGRI, F. R., RIBEIRO, A. M., NASIF, N., SOUZA-FILHO, J. P. and FERIGOLO, J. 2017. Tropical fossil caviomorph rodents from the southwestern Brazilian Amazonia in the context of the South American faunas: systematics, biochronology, and paleobiogeography. *Journal of Mammalian Evolution*, **24** (1), 57–70.

KOLARSKY, R. A., MANN, P. and MONTERO, W. 1995. Island arc response to shallow subduction of the Cocos Ridge, Costa Rica. *Special papers of the Geological Society of America*, **295**: 235–262.

LATRUBESSE, E. M., COZZUOL, M. A., SILVA-CAMINHA, S. A., RIGSBY, C. A., ABSY, M. L. and JARAMILLO, C., 2010. The late Miocene paleogeography of the Amazon Basin and the evolution of the Amazon River system. *Earth-Science Reviews*, **99**, 99–124.

LAURITO, C. A. and VALERIO, A. L. 2013. *Scirrotherium antelucanus*, una nueva especie de Pampatheriidae (Mammalia, Xenarthra, Cingulata) del Mioceno Superior de Costa Rica, América Central. *Revista Geológica de América Central*, **49**, 45–62.

LEIDY, J. 1889. Fossil Vertebrates from Florida. *Proceedings of the Academy of Natural Sciences of Philadelphia*, **41**: 96-97.

LOWERY, B. J. 1982. Sedimentology and tectonic implications of the Middle to Upper Miocene Curré Formation. Unpublished M.S. thesis, Louisiana State University, Baton Rouge, 100 pp.

LUND, P. 1839. Blik paa Braziliens Dyreverden for Sidste Jordomvaeltning. Anden Afhandling: Pattedyrene. *Det Kongelige Danske Videnskabernes SelskbasNaturvidenskabelige og Mathematiske Afhandlinger*, **8**: 61-144.

— 1842. Blik paa Braziliens Dyreverden for Sidste Jordomvaeltning. TredieAfhandling: Forsaettelse af Pattedyrene. *Det Kongelige Danske Videnskabernes SelskbasNaturvidenskabelige og Mathematiske Afhandlinger*, **8**: 217–272.

MACFADDEN, B. J. 2006. Extinct mammalian biodiversity of the ancient New World tropics. *Trends in Ecology & Evolution*, **21** (3), 157–165.

MADDISON, W. P. and MADDISON, D. R. 2010. Mesquite: a modular system for evolutionary analysis. Version 2.73. [http://mesquiteproject.org]

MARTINELLI, A. G., FERRAZ, P. F., CUNHA, G. C., CUNHA, I. C., DE SOUZA CARVALHO, I., RIBEIRO, L. C. B., MACEDO NETO, F., LOURENCINI CAVELLANI, C., ANTUNES TEIXEIRA, V. P. and DA FONSECA FERRAZ, M. L.

2012. First record of *Eremotherium laurillardi* (Lund, 1842) (Mammalia, Xenarthra, Megatheriidae) in the Quaternary of Uberaba, Triângulo Mineiro (Minas Gerais State), Brazil. *Journal of South American Earth Sciences*, **37**, 202–207.

MCDONALD, H. G. and LUNDELIUS, E. L., Jr. 2009. The giant ground sloth *Eremotherium laurillardi* (Xenarthra. Megatheriidae) in Texas. *In* ALBRIGHT, L.B., III (ed.), Museum of Northern Arizona, *Papers on geology, vertebrate paleontology, and biostratigraphy in honor of Michael O. Woodburne*, Bulletin **65**, 407–421.

MCKENNA, M.C. and BELL, S.K. 1997. *Classification of Mammals Above the Species Level*. Columbia University Press, New York, 640 pp.

MORENO, E. P. and MERCERAT, A. 1891. Exploración arqueológica de la provincia de Catamarca: Paleontología. *Revista del Museo de La Plata*, **1**: 222-236.

MORENO, F., HENDY, A. J. W., QUIROZ, L., HOYOS, N., JONES, D. S., ZAPATA, V., ZAPATA, S., BALLEN, G. A., CADENA, E., CÁRDENAS, A. L., CARRILLO-BRICEÑO, J. D., CARRILLO, J. D., DELGADO-SIERRA, D., ESCOBAR, J., MARTÍNEZ, J. I., MARTÍNEZ, C., MONTES, C., MORENO, J., PÉREZ, N., SÁNCHEZ, R., SUÁREZ, C., VALLEJO-PAREJA, M. C. and JARAMILLO, C. 2015. Revised stratigraphy of Neogene strata in the Cocinetas basin, La Guajira, Colombia. *Swiss Journal of Palaeontology*, **134** (1), 5–43.

OBANDO, L. G. 2011. Stratigraphic and tectonic of northeast part of Dota quadrangle (1: 50,000), Costa Rica. *Revista Geológica de América Central*, **44**: 71–82.

O'DEA, A., LESSIOS, H. A., COATES, A. G., EYTAN, R. I., RESTREPO-MORENO, S. A., CIONE, A. L., COLLINS, L. S., DE QUEIROZ, A., FARRIS, D. W., NORRIS, R.

D., STALLARD, R. F., WOODBURNE, M. O., AGUILERA, O., AUBRY, M-P., BERGGREN, W. A., BUDD, A. F., COZZUOL, M. A., COPPARD, S. E., DUQUE-CARO, H., FINNEGAN, S., GASPARINI, G. M., GROSSMAN, E. L., JHONSON K. G., LLOYD, D. K, KNOWLTON N., LEIGH E. G., LEONARD-PINGEL J. S., MARKO, P. B., PYENSON, N. D., RACHELLO-DOLMEN, P. G., SOIBELZON, E., SOIBELZON, L., TODD, J. A., VERMEIJ, G. J. and JACKSON, J. B. C. 2016. Formation of the Isthmus of Panama. *Science advances*, **2** (8), e1600883.

ORTIZ-JAUREGUIZAR, E. and CLADERA, G. A. 2006. Paleoenvironmental evolution of southern South America during the Cenozoic. *Journal of Arid Environments*, **66** (3), 498–532.

PATTERSON, B. and PASCUAL, R. 1968. The fossil mammal fauna of South America. *The Quarterly Review of Biology*, **43** (4), 409–451.

RIBEIRO, A. M., MADDEN, R. H., NEGRI, F. R., KERBER, L., HSIOU, A. S. and RODRIGUES, K. A. 2013. Mamíferos fósiles y biocronología en el suroeste de la Amazonia, Brasil. *In* BRANDONI, D. and NORIEGA, J.I. (eds.), *El Neógeno de la Mesopotamia argentina*, Asociación Paleontológica Argentina, Publicación Especial **14**, 207–221.

RINCÓN, A. D., SOLÓRZANO, A., BENAMMI, M., VIGNAUD, P. and MCDONALD, H. G. 2014. Chronology and geology of an Early Miocene mammalian assemblage in North of South America, from Cerro La Cruz (Castillo Formation), Lara State, Venezuela: Implications in the changing course of Orinoco River hypothesis. *Andean geology*, **41** (3), 507–528.

— — MACSOTAY, O., MCDONALD, H. G. and NÚÑEZ-FLORES, M. 2016. A new Miocene vertebrate assemblage from the Río Yuca Formation (Venezuela) and the northernmost record of typical Miocene mammals of high latitude (Patagonian) affinities in South America. *GeoBios*, **49** (5), 395–405.

RIVIER, F. 1985. Sección geológica del Pacífico al Atlántico a través de Costa Rica. *Revista Geológica de América Central*, **2**: 22–32.

ROBERTSON, J. S. 1976. Latest Pliocene mammals from Haile XV A, Alachua county, Florida. *Bulletin of the Florida State Museum, Biological Sciences*, **20**: 111–186.

SALAS-GISMONDI, R., FLYNN, J. J., BABY, P., TEJADA-LARA, J. V., WESSELINGH, F. P. and ANTOINE, P. O. 2015. A Miocene hyperdiverse crocodylian community reveals peculiar trophic dynamics in proto-Amazonian mega-wetlands. *Proceedings of the Royal Society B: Biological Sciences*, **282** (1804), 20142490.

SÁNCHEZ-VILLAGRA, M. R. 2012. Embryos in Deep Time: The Rock Record of Biological Development. University of California Press, Berkeley, California, 256 pp.

SCHMIDT, D. N. 2007. The closure history of the Panama Isthmus: evidence from isotopes and fossils to models and molecules. *In* WILLIAMS, M., HAYWOOD, A. M., GREGORY J., F. and SCHMIDT, D. N. (eds), *Deep time perspectives on climate change – marrying the signal from computer models and biological proxies*. Geological Society of London, London, pp. 427–442.

SCILLATO-YANÉ, G. J., CARLINI, A. A., TONNI, E. P. and NORIEGA, J. I. 2005. Paleobiogeography of the late Pleistocene pampatheres of South America. *Journal of South American Earth Sciences*, **20** (1–2), 131–138.

— GÓIS, F., ZURITA, A. E., CARLINI A. A., GONZÁLEZ RUIZ, L. R., KRMPOTIC, C. M., OLIVA, C. and ZAMORANO, M. 2013. Los Cingulata (Mammalia, Xenarthra) del "Conglomerado Osífero" (Mioceno tardío) de la Formación Ituzaingó de Entre Ríos, Argentina. *In* BRANDONI, D. and NORIEGA, J.I. (eds.), *El Neógeno de la Mesopotamia argentina*, Asociación Paleontológica Argentina, Publicación Especial **14**, 118–134.

SIGOVINI, M., KEPPEL, E. and TAGLIAPIETRA, D. 2016. Open Nomenclature in the biodiversity era. *Methods in Ecology and Evolution*, **7** (10), 1217–1225.

SIMPSON, G. G. 1930. *Holmesina septentrionalis*, extinct giant armadillo of Florida. *American Museum Novitates*, **442**: 1–10.

SILVA, J. C., PARDO, A., CARDONA, A., BORRERO, C., FLORES, A., NAVARETTE, R., MEJÍA, A., OCHOA, D., OSORIO, J. A., ROSERO, S. and ARENAS, A. 2012. Multi-Chronological Proxies to Timing Early Oligocene and Middle Miocene Deformation Events Along the Lower Magdalena Basin, NW Colombia. *Resúmenes del XI Simposio Bolivariano-Exploración Petrolera en las Cuencas Subandina*s, Asociación Colombiana de Geólogos y Geofísicos del Petróleo. [http://www.earthdoc.org/publication/publicationdetails/?publication=66175]

STIRTON, R. A. 1953. Vertebrate paleontology and continental stratigraphy in Colombia. *Geological Society of America Bulletin*, **64** (6), 603–622.

SWOFFORD, D. L. 2015. PAUP*: Phylogenetic analysis using parsimony (and other methods) (version 4.0a142).

1398 — and BELL, C. D. 2017. PAUP* manual. Available at http://phylosolutions.com/paup-
1399 documentation/paupmanual.pdf.

1400 TITO, G. 2008. New remains of *Eremotherium laurillardi* (Lund, 1842) (Megatheriidae,
1401 Xenarthra) from the coastal region of Ecuador. *Journal of South American Earth*
1402 *Sciences*, **26** (4), 424–434.

1403 VILLARROEL, C. and CLAVIJO, J. 2005. Los mamíferos fósiles y las edades de las
1404 sedimentitas continentales del Neógeno de la Costa Caribe Colombiana. *Revista de la*
1405 *Academia Colombiana de Ciencias*, **29** (112), 345–356.

1406 VIZCAÍNO, S. F., DE IULIIS, G. and BARGO, M. S. 1998. Skull shape, masticatory
1407 apparatus, and diet of *Vassallia* and *Holmesina* (Mammalia: Xenarthra:
1408 Pampatheriidae): when anatomy constrains destiny. *Journal of Mammalian Evolution*, **5**
1409 (4), 291–322.

1410 WEBB, S. D. 2006. The Great American Biotic Interchange: Patterns and Processes.
1411 *Annals of the Missouri Botanical Garden*, **93** (2), 245–258.

1412 WOODBURNE, M. O. 2010. The Great American Biotic Interchange: dispersals, tectonics,
1413 climate, sea level and holding pens. *Journal of Mammalian Evolution*, **17** (4), 245–264.

1414 — and SWISHER, C. C. III. 1995. Land mammal high-resolution geochronology,
1415 intercontinental overland dispersals, sea level, climate and vicariance. *In* BERGGREN,
1416 W. A., KENT, D. W., AUBRY, M.-P. and HARDENBOL, J. (eds.), *Geochronology,*
1417 *Time Scales and Global Stratigraphic Correlation*. *SEPM Special Publication*, **54**, 335-
1418 364.

— CIONE, A. L. and TONNI, E. P. 2006. Central American provincialism and the Great American Biotic Interchange. Universidad Nacional Autónoma de México, Instituto de Geología y Centro de Geociencias, *Publicación Especial*, **4**, 73–101.

YUAN, P. B. 1984. Stratigraphy, sedimentology and geologic evolution of eastern Terraba Trough, southwestern Costa Rica. Unpublished PhD thesis, Louisiana State University, Baton Rouge, 110 pp.

ZURITA, A. E., SCILLATO-YANÉ, G. J., CIANCIO, M., ZAMORANO, M. and GONZÁLEZ-RUIZ, L. R. 2016. Los Glyptodontidae (Mammalia, Xenarthra): Historia biogeográfica y evolutiva de un grupo particular de mamíferos acorazados. *Contribuciones del MACN*, **6**, 249-262.

FIGURE CAPTIONS

Figure 1. Geographical and stratigraphic provenance of the newly described material of pampatheriids from the Neogene of Colombia. In the left upper corner, a map of northwesternmost South America and the location of the regions of Colombia where there are outcrops of the formations with pampatheriid specimens for this study. In the right upper corner, photos of characteristic outcrops of these formations. Below in the center, a general chronostratigraphic scheme with the position of each formation within the Neogene and two important tectonic/palaeogeographical events in northwestern South America, i.e. a major, underwater uplift of the Isthmus of Panama (Schmidt 2007) and the definitive emergence of the Panama Land Bridge (O'dea et al. 2016). The photo of outcrops of the Castilletes Formation was taken by Edwin Cadena.

1441 **Figure 2.** Phylogenetic results. A, strict consensus tree of the parsimony with equal
1442 weights. Numbers below nodes are absolute Bremer support values. B, strict consensus tree
1443 of the parsimony analysis with implied weights. C, majority-rule consensus tree of the
1444 bootstrap resampling with implied weights. The numbers below nodes are bootstrap
1445 support values. Note the difference in the phylogenetic position of *Holmesina floridanus* in
1446 the two strict consensus trees. Explanation of this difference in the main text.

1447 **Figure 3.** Fixed and (semi) mobile osteoderms of *Scirrotherium hondaensis* from the La
1448 Victoria and Villavieja Formations, Municipality of Villavieja, Department of Huila,
1449 Colombia. A–B', fixed osteoderms; C'–K', (semi) mobile osteoderms. The osteoderms G,
1450 J, K, L, W, X, Y, Z, A', B', G', I', J' and K' are associated with the catalog number VPPLT
1451 348. The osteoderms H, U and V are associated with the catalog number VPPLT 004. The
1452 osteoderms T and D' are associated with the catalog number VPPLT 701. All the former
1453 osteoderms come from the lower and middle La Victoria Formation. The osteoderms B, C,
1454 F, I, O, P, S, C' and F' are associated with the catalog number VPPLT 1683 - MT 18 and
1455 come from the top of the La Victoria Formation. The osteoderms A, D, E, M, N, Q, R, E'
1456 and H' are associated with the catalog number VPPLT 1683 - MT 18 and come from the
1457 lower Villavieja Formation. Scale bar equal to 20 mm.

1458 **Figure 4.** Photos and anatomical line drawings of the skull VPPLT 706 of *Scirrotherium*
1459 *hondaensis* from the middle La Victoria Formation, Municipality of Villavieja, Department
1460 of Huila, Colombia. A–B, dorsal views; C–D, ventral views; E–F, right lateral views; D–H,
1461 left lateral views. *Abbreviations*: aof, antorbital fossa; fr, frontals; iof, infraorbital foramen;
1462 j, jugal; la, lacrimal; Mf1, first upper molariform; Mf9, ninth upper molariform; mx,

maxilla; mxf, maxillary foramen; na, nasals; pal, palatines; pm, premaxilla. Scale bar equal to 50 mm.

Figure 5. Photos and anatomical line drawings of the left femur and right ulna VPPLT 706 of *Scirrotherium hondaensis* from the middle La Victoria Formation, Municipality of Villavieja, Department of Huila, Colombia. The epiphyses of this femoral diaphysis have been reconstructed from those with catalog number UCMP 39846. A–B, anterior views of the femur; C–D, posterior views of the femur. E–F, medial views of the ulna; G–H, lateral views of the ulna. *Abbreviations*: anc, fossa for the anconeus muscle; cp, coronoid process; fh, femoral head; gt, greater trochanter; le, lateral epicondyle; me, medial epicondyle; op, olecranon process; tn, trochlear notch; tt, third trochanter. Scale bar equal to 50 mm.

Figure 6. Photos and anatomical line drawings of a thoracic vertebra (A–B) and several anterior caudal vertebrae (C–F) VPPLT 706 of *Scirrotherium hondaensis* from the middle La Victoria Formation, Municipality of Villavieja, Department of Huila, Colombia. A–B, posterior views of the thoracic vertebra. C–D, lateral views of caudal vertebrae; E–F, dorsal views of caudal vertebrae. *Abbreviations*: az, anterior zygapophyses; mp, metapophyses; ns, neural spine; tp, transverse processes; vb, vertebral body; vla, ventrolateral apophyses. Scale bar equal to 30 mm.

Figure 7. Photos and anatomical line drawings of the astragalus (A–D) and calcaneum (E – F) UCMP 39846 of *Scirrotherium hondaensis* from the lower (?) Villavieja Formation, Municipality of Villavieja, Department of Huila, Colombia. A–B, astragalus in plantar views; C–D, astragalus in dorsal views. E–F, calcaneum in dorsal views. *Abbreviations*: ct, calcaneal tuber; ef, ectal facet; h, head of the astragalus; lt, lateral trochlea; mf, medial trochlea; sf, sustentacular facet; st, *sulcus tali*. Scale bar equal to 20 mm.

1486 **Figure 8.** Fixed osteoderm MUN STRI 36880 of *Scirrotherium antelucanus* from the upper
1487 Sincelejo Formation, Municipality of Los Palmitos, Department of Sucre, Colombia. Scale
1488 bar equal to 20 mm.

1489 **Figure 9.** Osteoderms referred to aff. *Scirrotherium* (**A**, MUN STRI 16718; **E**, MUN STRI
1490 38064; and **G,** MUN STRI 16719; all these specimens are from the Castilletes Formation
1491 and they are fixed osteoderms except the latter, which consist of an anterior fragment of a
1492 mobile osteoderm); *Scirrotherium* cf. *hondaensis* (**C**, MUN STRI 36814, a fixed osteoderm
1493 from the Castilletes Formation); and *Scirrotherium* sp. (**B**, MUN STRI 36801; **D**, MUN
1494 STRI 16158; and **F**, MUN STRI 34373; all these osteoderms are from the Castilletes
1495 Formation, except the latter, which comes from the Ware Formation); Municipality of
1496 Uribia, Department of La Guajira, Colombia. Note the two well-developed rows of anterior
1497 foramina in the osteoderms MUN STRI 16718 and 38064. Scale bar equal to 20 mm.

1498 **Figure 10.** Osteoderms of *Kraglievichia carinatum* comb. nov. from the Ituzaingó
1499 Formation, Entre Ríos Province, Argentina. The holotype of this species is marked with
1500 one single asterisk (*) and paratypes with double asterisk (**). A–J, fixed osteoderms; K–
1501 R, (semi) mobile osteoderms. **A**, MLP 69-IX-8-13AC**; **B**, MLP 70-XII-29-1**; **C**, MLP
1502 41-XII-13-905; **D**, MLP 69-IX-8-13AF; **E**, MLP 69-IX-8-13AG; **F**, MLP 41-XII-13-414A;
1503 **G**, MLP 69-IX-8-13AN; **H**, unknown catalog number; **I**, MLP 69-IX-8-13AK; **J**, MLP 41-
1504 XII-13-414B; **K**, MLP 69-IX-8-13AS; **L**, MLP 69-IX-8-13AE**; **M**, MLP 52-X-1-36; **N**,
1505 MLP 69-IX-8-13AB*; **O**, MLP 41-XII-13-909; **P**, MLP 69-IX-8-13AW; **Q**, MLP 69-IX-8-
1506 13AQ; **R,** MLP 69-IX-8-13AY. Scale bar equal to 20 mm.

1507 **Figure 11.** One outstanding morphological difference between typical osteoderms of
1508 *Scirrotherium* and *Kraglievichia*: Uniformly narrow LCE in fixed osteoderms of

Scirrotherium (left; *S. hondaensis*); and anteriorly wide, posteriorly tapered LCE in the same osteoderms of *Kraglievichia* (right; *K. carinatum* comb. nov.). Not to scale.

Figure 12. Time-calibrated phylogeny of the clade *Scirrotherium* + *Kraglievichia* + *Holmesina* based on the strict consensus cladogram from this work (Fig. 2). Polytomies from the strict consensus tree (Fig. 2B) were resolved by (1) forcing the monophyly of *S. hondaensis* and *S. antelucanus* and (2) placing the species *H. septentrionalis* and *H. occidentalis* as successively basal to the largest South American *Holmesina* species, i.e. *H. paulacoutoi* and *H. major*. Note the diversification events of the clade *Scirrotherium* + *Kraglievichia* + *Holmesina* are mainly concentrated during the Burdigalian (late Early Miocene) and Plio-Pleistocene. Likewise, note the relative long ghost lineage of *Holmesina*. Images of the pampatheriids are from *PhyloPic* (all available under public domain): top, *Pampatherium humboldtii* (http://phylopic.org/name/670230e9-4775-493c-b3ab-31718fb570a3); below, *Holmesina floridanus* (http://phylopic.org/name/73635941-ed8a-4518-aae8-70e824dbee97).

Figure 13. Geographical distributions and intercontinental dispersal events of the clade *Scirrotherium* + *Kraglievichia* + *Holmesina* during the Neogene-Pleistocene. The symbols (i.e. squares, circles and triangles) should not necessarily be interpreted as single localities but as approximate areas of occurrence. This is especially true for the Pliocene and Pleistocene epochs.

TABLES

Table 1. Fixed (scapular and pelvic) osteodermal measurements for taxa of interest in this study.

Taxon/Measurement	Length	Width	Thickness	References
S. hondaensis	16-35.2	17.5-27.9	3.7-6.9	This work; Góis et al. 2013
S. antelucanus	28.6-40.9	22-32.4	4.9-7.1	This work; Laurito & Valerio 2013
K. carinatum comb. nov.	20.9-33.5	17-26.1	4.1-5.9	This work; Góis et al. 2013
K. paranensis	30-45	22.5-28.3	6-11	Góis et al. 2013
H. floridanus	24.4-36.7	18.9-32.1	6-9.7	This work; Edmund 1987

Table 2. Mobile and semi-mobile osteodermal measurements for taxa of interest in this study.

Taxon/Measurement	Length	Width	Thickness	References
S. hondaensis	29.4-60	17.9-27.4	4.9-7.3	This work; Góis et al. 2013
S. antelucanus	38.2-64.6	19.4-28.9	-	Laurito & Valerio 2013
K. carinatum comb. nov.	32-54.5	17-28.9	3.9-6	This work; Góis et al. 2013
K. paranensis	60.5-70.5	25-29	7-9	Góis et al. 2013
H. floridanus	61.8-71	17.6-28.5	4.7-6.3	This work; Edmund 1987

Table 3. Selected cranial measurements for the specimen VPPLT 706 of *Scirrotherium hondaensis* and related taxa whose skulls are known.

Taxon/Measurement	GSL	NL	FL	PAL	LUR	PL	References
S. hondaensis	117.3*	~52.8	~55	-	84.1	94.3	This work
K. cf. *paranensis*	194	58	62	74	-	159	This work
*H. floridanus***	249	106.3	75	58.6	133.6	185	This work
H. septentrionalis	290	-	-	-	165	220	Góis et al. 2012

*Incomplete

**Specimen UF 191448

Table 4. Femoral measurements for *Scirrotherium hondaensis* and related taxa whose femur is known.

Measurement/Taxon	GFL	TTW	DW	References
S. hondaensis	162*	27.6	32.5	This work
K. cf. *paranensis*	164	33.7	38	This work
*H. floridanus***	195	41	47	This work
H. septentrionalis	290	70	86	Góis 2013

*Estimated from the specimens VPPLT 706 and UCMP 39846

**Specimen UF 24918

Figure 1

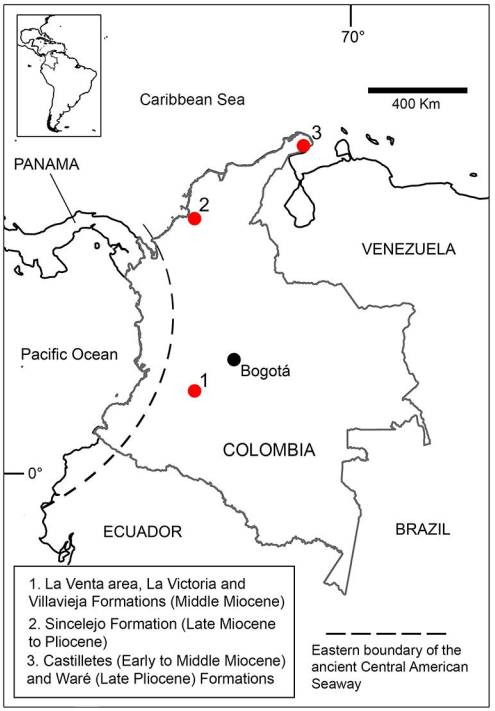

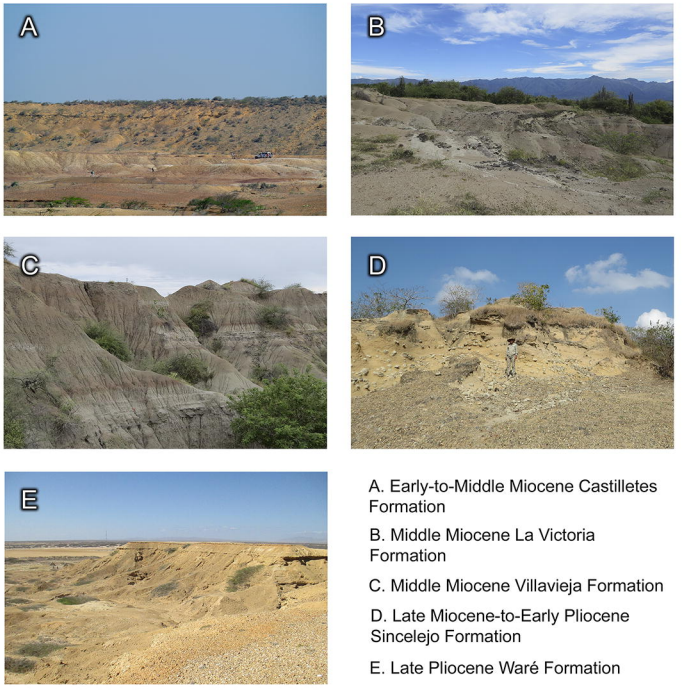

A. Early-to-Middle Miocene Castilletes Formation

B. Middle Miocene La Victoria Formation

C. Middle Miocene Villavieja Formation

D. Late Miocene-to-Early Pliocene Sincelejo Formation

E. Late Pliocene Waré Formation

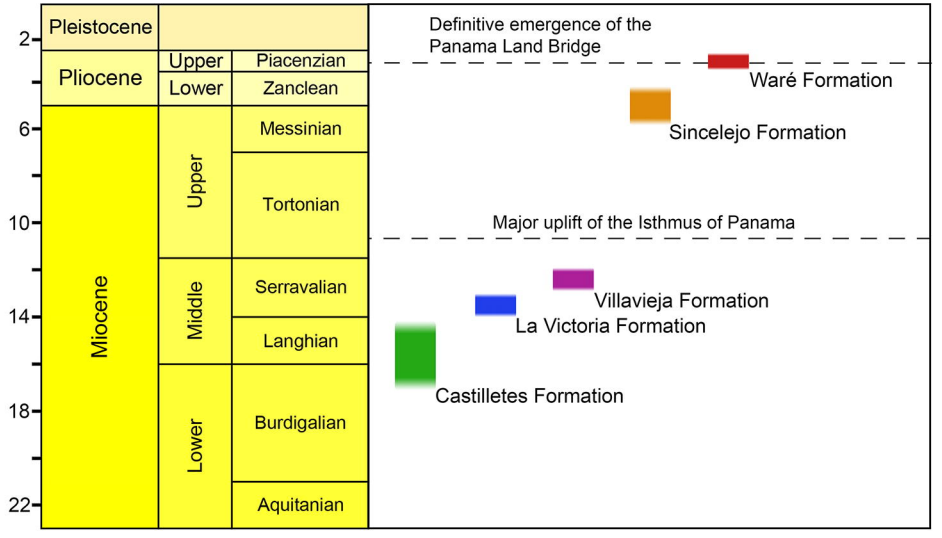

Figure 2

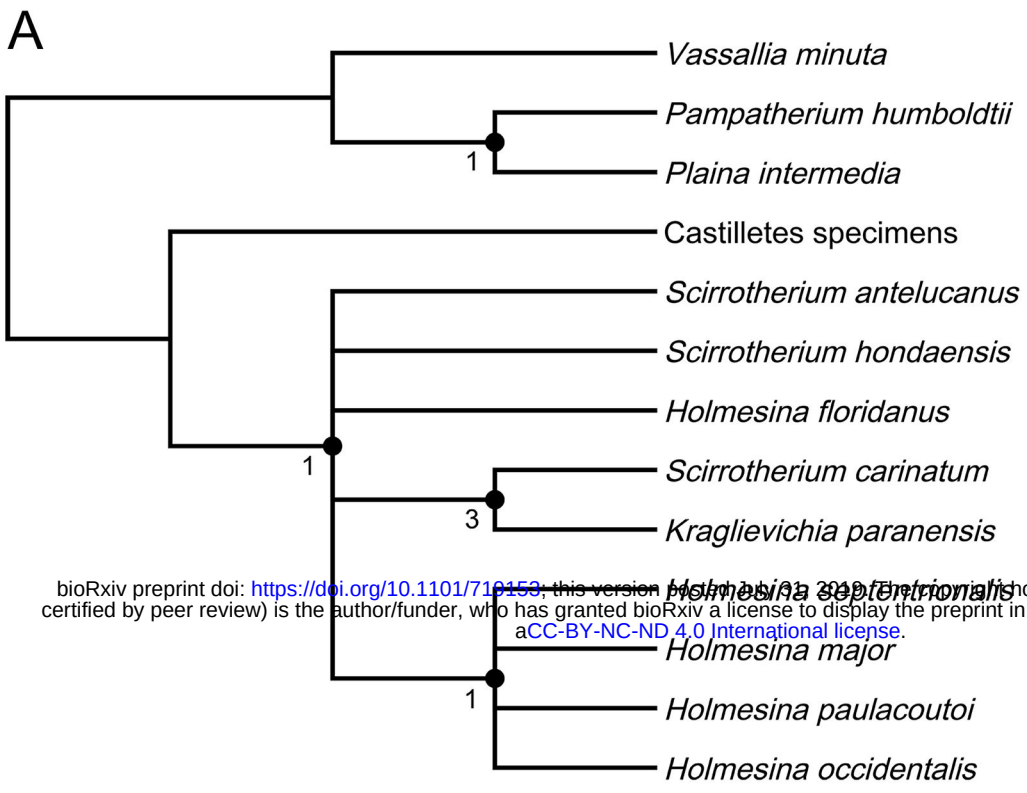

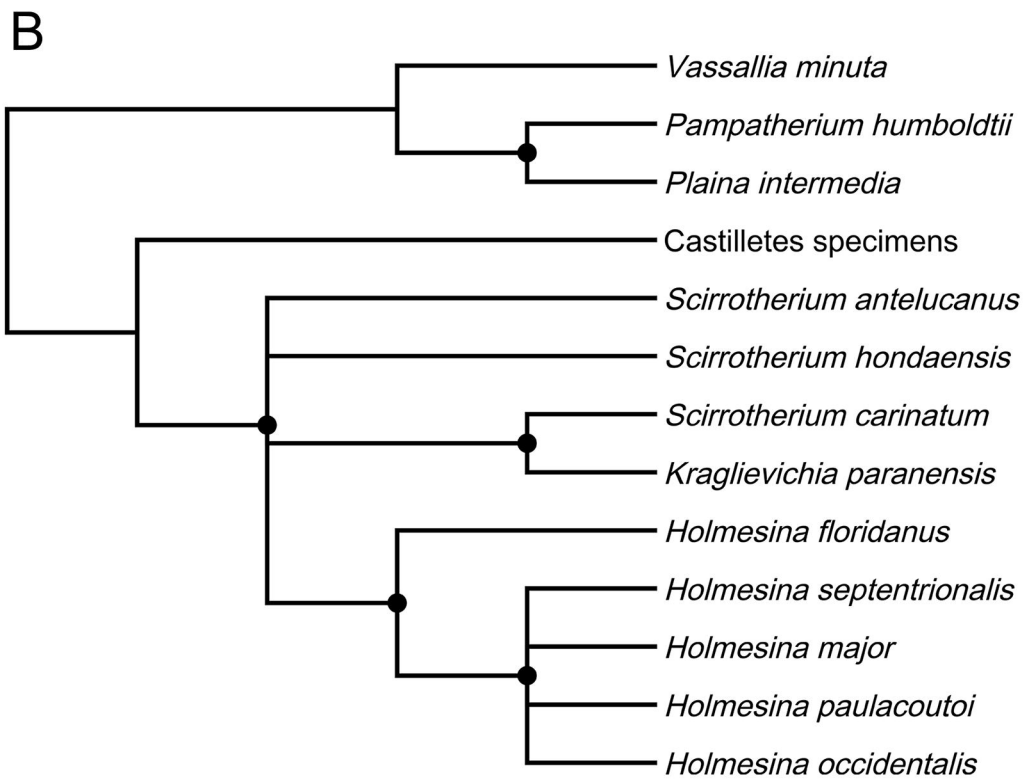

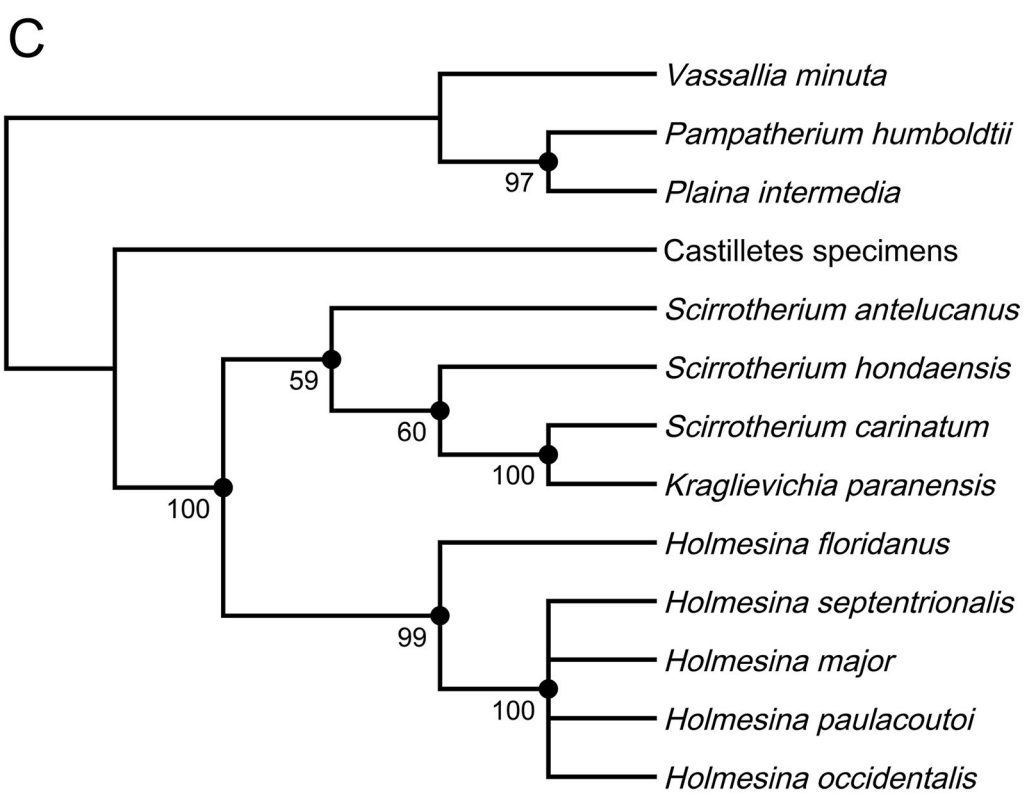

Figure 3

Figure 4

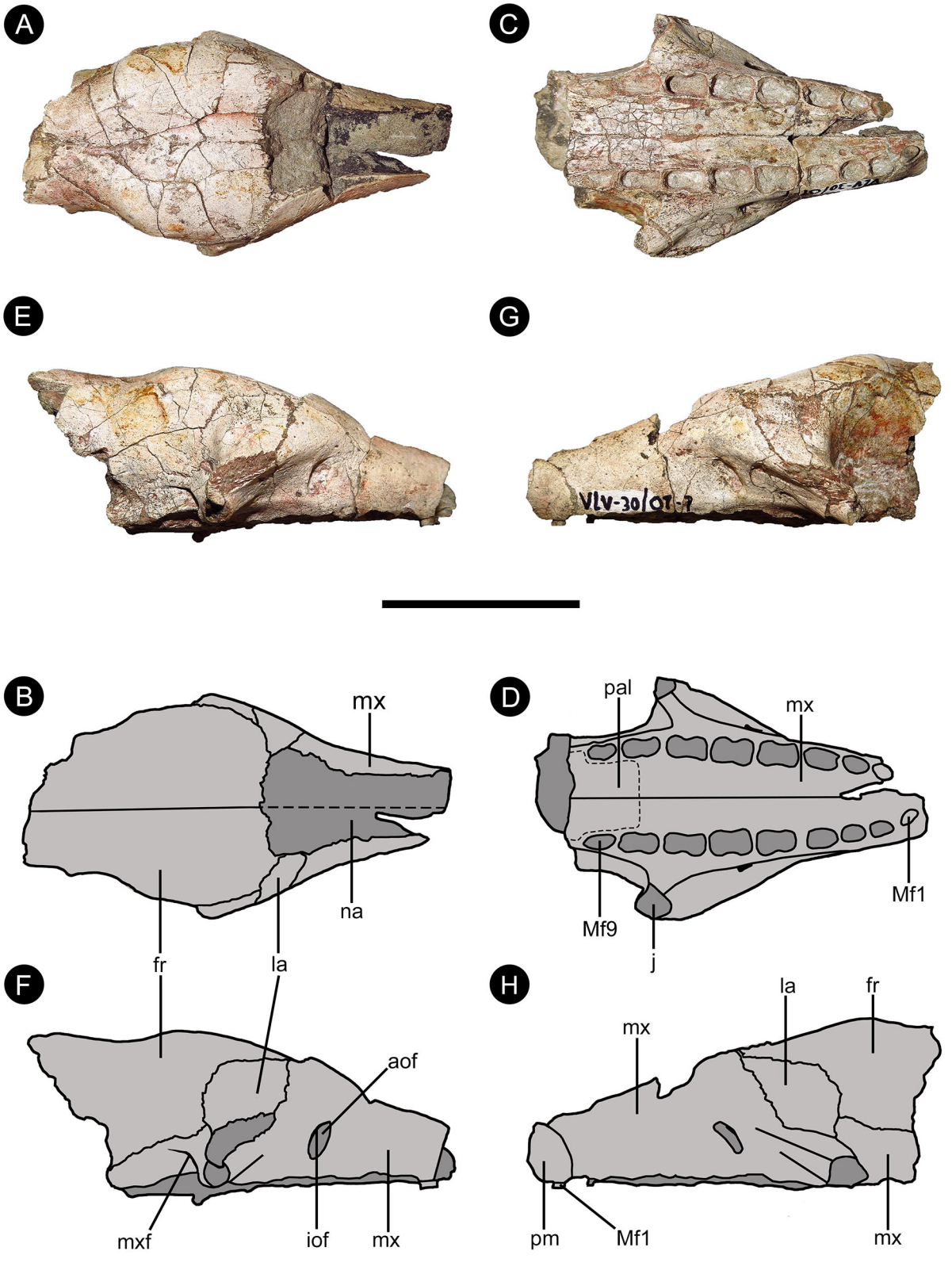
A
C
E
G
VLV-30/OT-7
B
mx
na
fr
la
D
pal
mx
Mf1
Mf9
j
F
aof
mxf
iof
mx
H
la
fr
mx
pm
Mf1
mx

Figure 5

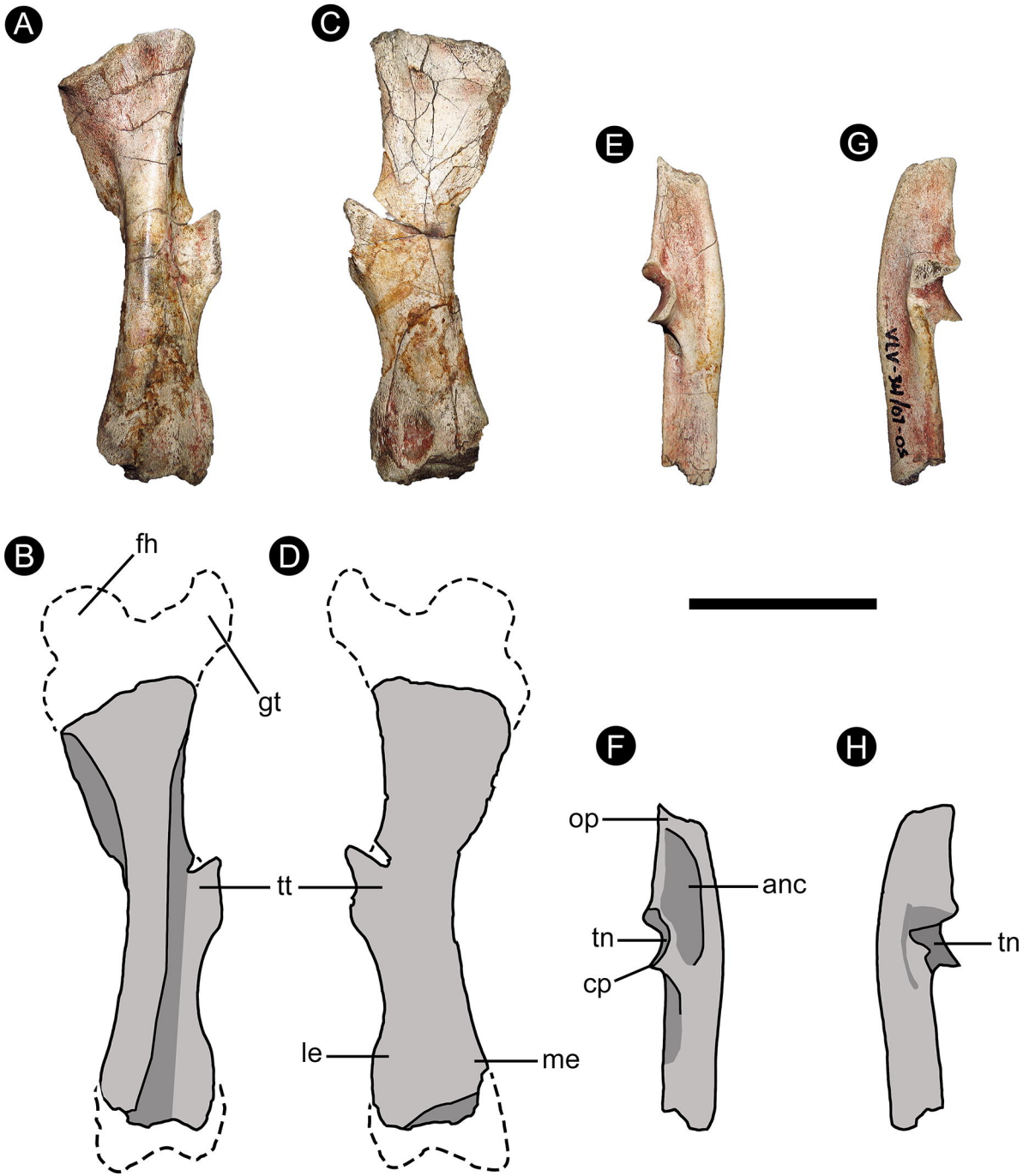

Figure 6

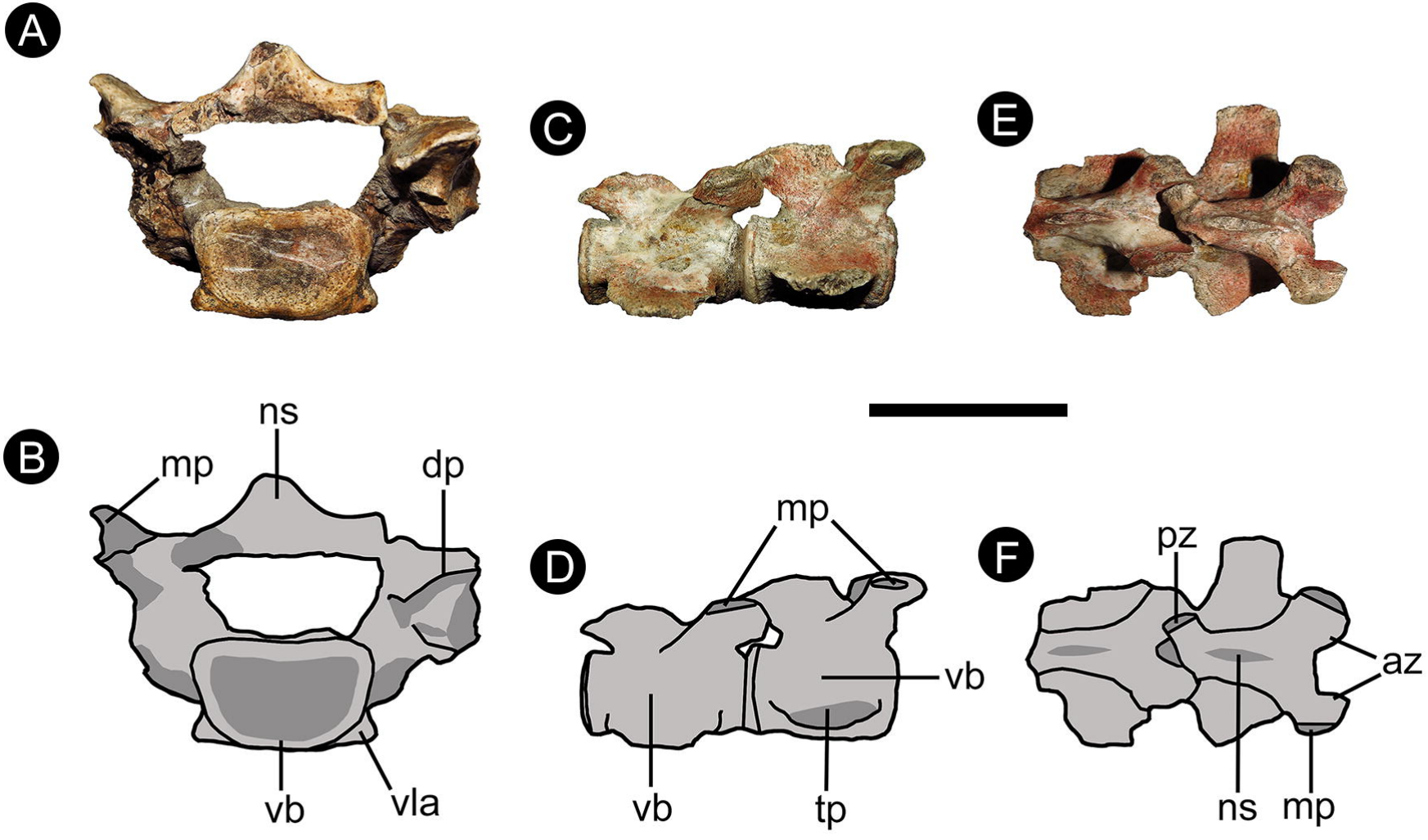

Figure 7

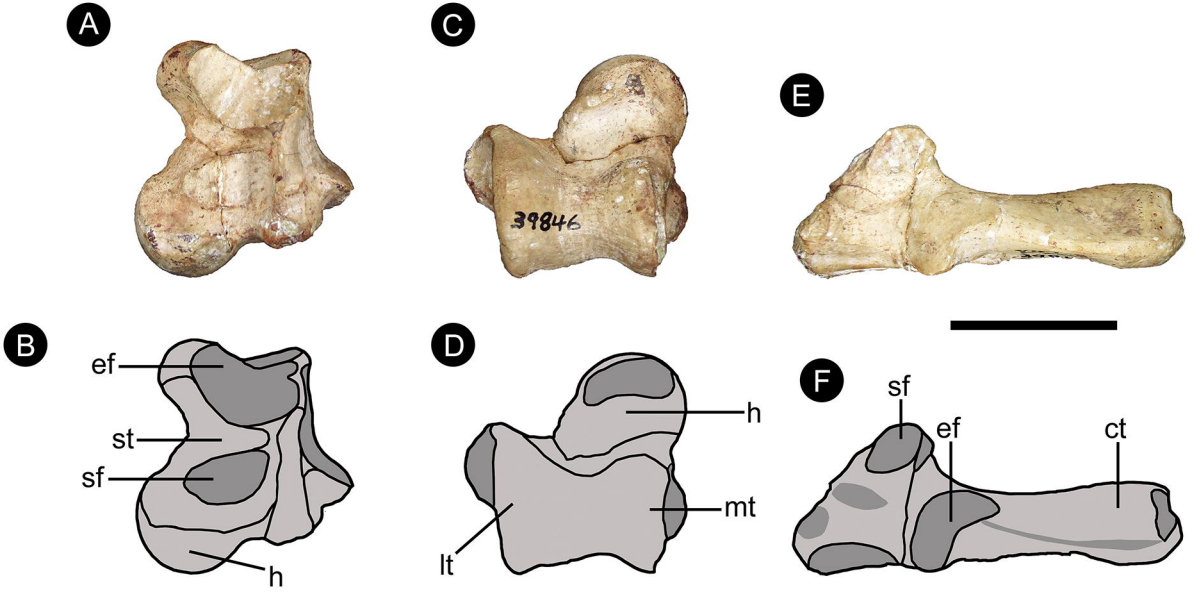

Figure 8

Figure 9

Figure 10

Figure 11

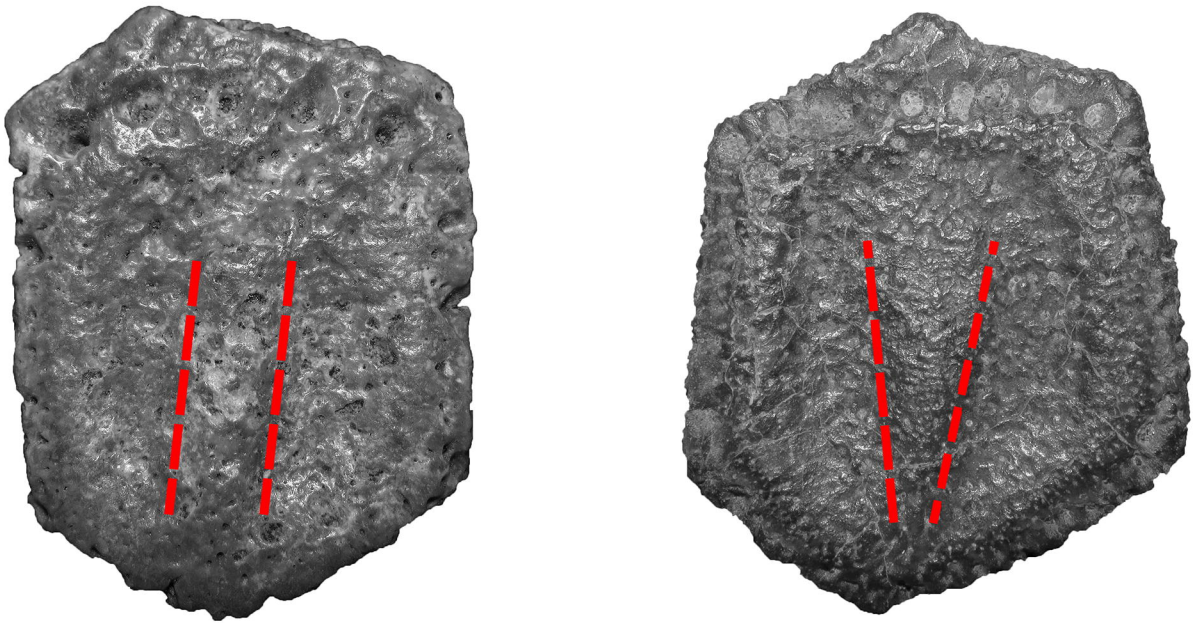

Figure 12

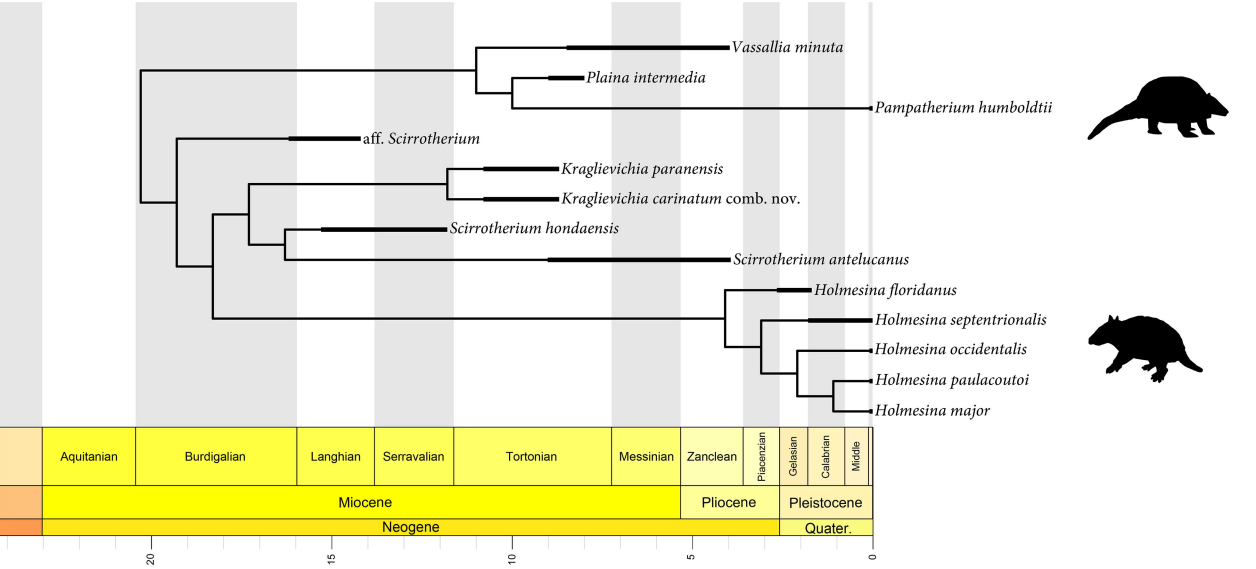
Vassallia minuta
Plaina intermedia
Pampatherium humboldtii
aff. Scirrotherium
Kraglievichia paranensis
Kraglievichia carinatum comb. nov.
Scirrotherium hondaensis
Scirrotherium antelucanus
Holmesina floridanus
Holmesina septentrionalis
Holmesina occidentalis
Holmesina paulacoutoi
Holmesina major
Aquitanian
Burdigalian
Langhian
Serravalian
Tortonian
Messinian
Zanclean
Piacenzian
Gelasian
Calabrian
Middle
Miocene
Pliocene
Pleistocene
Neogene
Quater.
20
15
10
5
0

Figure 13